## Temperature-driven vapor pressure deficit structures forest

bryophyte communities across the landscapes

Anna Růžičková 1,2, Matěj Man 1,2, Martin Macek 1, Jan Wild 1, Martin Kopecký 1

- 4 Institute of Botany of the Czech Academy of Sciences, Zámek 1, Průhonice, CZ-252 43, Czech Republic,
- <sup>2</sup> Department of Botany, Faculty of Science, Charles University, Benátská 2, Prague 2, CZ-128 00, Czech Republic
- 6 Correspondence to: Anna Růžičková (anna.ruzickova @ibot.cas.cz), Martin Kopecký (ma.kopecky@gmail.com)

#### Abstract

3

- 8 Atmospheric vapor pressure deficit (VPD) controls local plant physiology and global vegetation productivity.
- 9 However, at ecologically crucial intermediate spatial scales, the processes controlling VPD variability and the role
- of this VPD variability in forest bryophyte community assembly and the processes controlling this variability are
- 11 little known.
- 12 To explore VPD effects on bryophyte community composition and richness and to disentangle processes
- 13 controlling landscape-scale VPD variability-and explore VPD effects on bryophyte community composition and
- 14 richness, we recorded bryophyte communities and simultaneously measured forest microclimate air temperature
- and relative humidity across a topographically diverse landscape representing a bryophyte diversity hotspot
- in temperate Europe. Based on VPD importance for plant physiology, we hypothesize that VPD can be an
- 17 important also for bryophyte community assembly and that VPD variability will be jointly driven by saturated
- and actual vapor pressure across the topographically diverse landscape with contrasting forest types and steep
- 19 microclimatic gradients.
- 20 Contrary to our expectation, VPD variability in the forest understory was dictated by temperature-driven
- 21 differences in saturated vapor pressure, while actual vapor pressure was surprisingly constant across the landscape.
- 22 Gradients in bryophyte community species composition, and species richness and community structure of
- 23 bryophyte assemblages followed closely the VPD variability. The average daily mean VPD was much better
- 24 predictor of species composition than average daily maximum VPD and the mean VPD also explained significantly
- 25 more variation in species composition and richness than maximum temperature, indicating that time-averaged
- 26 evaporative stress is more relevant for bryophyte communities than microclimatic extremes. While mesic forest
- 27 bryophytes occurred along the whole VPD gradient, azonally species occurring near their distributional limits and
- 28 locally rare species preferred sites with low VPD. In result, low VPD sites represent species-rich microclimatic
- 29 refugia within the landscape, whereand host regionally abundant mesic forest bryophytes simultaneously coexist
- with rare species occurring near their distributional range limits.
- 31 Our results showed that VPD variability at ecologically crucial landscape scales is controlled
- 32 by temperature-driven saturated vapor pressure and consequently by the maximum air temperature. Future climate
- 33 warming will thus increase evaporative stress and reshuffle VPD-sensitive forest bryophyte communities even
- 34 in topographically diverse landscapes, which are traditionally considered as microclimatic refugia <u>buffered against</u>
- 35 <u>climate change</u>. Azonally Bryophyte species occurring near their distributional range limits rare bryophyte species
- 36 and therefore concentrated in low VPD sites will be especially vulnerable to the future changes in atmospheric
- 37 VPD.

#### 1. Introduction

38

39

40 41

42

43

44

45

46

47

48

49

50

51

52

53

54

55

56

57

58

59

60

61

62

63

64

65

66

67

68

69

70

71

72

73

74

75

76

77

Vapor pressure deficit (VPD) expresses atmospheric water demand as the difference between the amount of water vapor the air can hold at a given temperature and the actual amount of water vapor present in the air. Unlike relative air humidity, VPD accurately expresses plant evaporative stress (Campbell & Norman 1997). Since air capacity to hold water vapor increases exponentially with temperature, the same relative humidity at different temperatures indicates very different atmospheric moisture conditions (Anderson, 1936). An atmosphere with the same relative air humidity may be very "dry" (when the temperature is high) or it may be very "wet" (when the temperature is low). Relative air humidity therefore does not indicate the atmospheric moisture condition in physiologically meaningful way, despite its popularity in ecological studies (Campbell & Norman 1997). In contrast, VPD directly expresses the atmospheric moisture conditions in terms of plant evaporative stress (Anderson, 1936). Atmospheric vapor pressure deficit (VPD) is a key driver of plant functioning in terrestrial ecosystems (Ruehr et al., 2014; Grossiord et al., 2020)., because hHigher VPD means higher evaporative stress for plants, which-leads to reduced photosynthesis in the short term and drought-induced mortality in the long term (McDowell et al., 2008; Fu et al., 2022). Ongoing climate changes further exacerbate this VPD-driven evaporative stress because higher temperatures lead to an exponential increase in VPD (Lawrence, 2005; Grossiord et al., 2020). Increasing atmospheric VPD already limits global vegetation productivity (Yuan et al., 2019; López et al., 2021; Lu et al., 2022) and triggers large-scale forest diebacks (Breshears et al., 2013; Eamus et al., 2013; Williams et al., 2013). Yet, iIn contrast to the widely recognized role of VPD effects onin local plant physiology and global vegetation functioning, VPD effects on plant community assembly are largely unknowthe understanding of the processes that control landscape-scale VPD variability nand the effects of this variability on plant community assembly is limited (Novick et al., 2024). The knowledge about VPD effects on plant communities and the processes that control VPD variability over the landscape are Yet this knowledge is crucial for more realistic predictions of climate change impacts on vegetation and the identification of microclimatic refugia (Ashcroft and Gollan, 2013; Davis et al., 2019; Finocchiaro et al., 2024; Ogée et al., 2024). Because VPD is a difference between saturated vapor pressure (Psat) and actual vapor pressure (Pair), VPD variability across space reflects the complex interplay between spatial patterns in saturated and actual vapor pressures. While saturated vapor pressure (Pset) is controlled solely an exponential function ofby air temperature, actual vapor pressure (Pair) is influenced by many processes operating at different spatial scales - ranging from regional atmospheric circulation and precipitation to local evaporation from soil and water surfaces and plant transpiration (Campbell and Norman, 1998). Yet, despite increasingly recognized VPD importance, it is still unknown how these contrasting processes integrate into the resulting VPD variability over the landscape is still unknown. A deeper understanding of the mechanisms behind landscape-scale VPD variability is particularly important for climate change biology. Scientists predict a temperature increase of up to 4.4 °C by 2100 (IPCC, 2023), which would lead to a more than 40 % increase in VPD for the same atmospheric water vapor content (Will et al., 2013). These changes can also modify VPD variability over the landscape, and therefore potentially change shift the distribution of individual species and therefore alter the composition of plant communities. However, VPD effects on plant distribution and community assembly over the landscape are not sufficiently known. Among plants, bryophytes are exceptionally sensitive to evaporative stress because they lack roots, lignified

water-conducting system, water storage tissues, and active stomata and have a large surface area in proportion to

78 biomass (Rice et al., 2001, Goffinet and Shaw, 2009). When exposed to the air with non-zero VPD, bryophytes 79 therefore inevitably lose water (Hinshiri and Proctor, 1971; Busby and Whitfield, 1978). Because bryophytes transport water only passively, mainly through external capillary spaces between tiny parts of their body 80 (Schofield, 1981), and their internal water content is thus a function of the water availability in the surrounding 81 82 environment (Vanderpoorten and Goffinet, 2009). Once the external water evaporates, bryophyte cells rapidly lose 83 turgor, metabolic activity slows down, and carbon fixation decreases. 84 To cope with this evaporative stress When this water evaporates, bryophytes developed evolutionary and 85 ecologically unique desiccation strategy, allowing them toean survive drought episodes in a desiccated state 86 (Proctor, 2000, 2001). Despite this unique bryophyte ability to survive microclimatic extremestolerate desiccation, 87 bryophyte assemblages are potentially highly sensitive to evaporative stress, because desiccation tolerance widely 88 differs among bryophyte species (Hinshiri and Proctor, 1971; Wagner and Titus, 1984, Oliver et al., 2000; Proctor, 89 Ligrone, et al., 2007; Proctor, Oliver, et al., 2007). Therefore, it can be assumed that the atmospheric VPD – an 90 ecologically meaningful variable expressing evaporative stress – will strongly affect composition, richness and 91 structure of bryophyte assemblages. Yet surprisingly little is known about the VPD effect on bryophyte 92 assemblages in temperate forests (Fenton and Frego, 2005). 93 To provide this missing knowledge, Here we combined detailed in-situ forest microclimate measurements with 94 simultaneous bryophyte inventories conducted across topographically diverse landscape representing bryophyte 95 diversity hotspot in central Europe to provide this missing knowledge. Specifically Using these data, we explored 96 how landscape-scale VPD variability affects bryophyte community composition and species richness in temperate 97 forests, quantified VPD variability over the topographically diverse landscape, and identified which processes 98 drive this variability, and explored how landscape scale VPD variability affects bryophyte community 99 composition and species richness in temperate forests.

#### 2. Material and methods

#### 2.1 Study area

100

101

102

103

104

105

106

107

We recorded bryophytes and measured microclimate in the Bohemian Switzerland National Park in the Czech Republic (Fig. 1). The rugged terrain of this sandstone landscape creates a fine-scale mosaic of contrasting habitats with steep microclimatic gradients over short distances (Wild et al., 2013). The elevation within the national park ranges from 125 to 619 m<sub>2</sub> and the mean elevation is 340 m. According to the data from the Tokáň weather station (Fig. 1), the mean annual air temperature during the 2011-2019 period was 8.3 °C, and the mean annual precipitation was 765 mm.

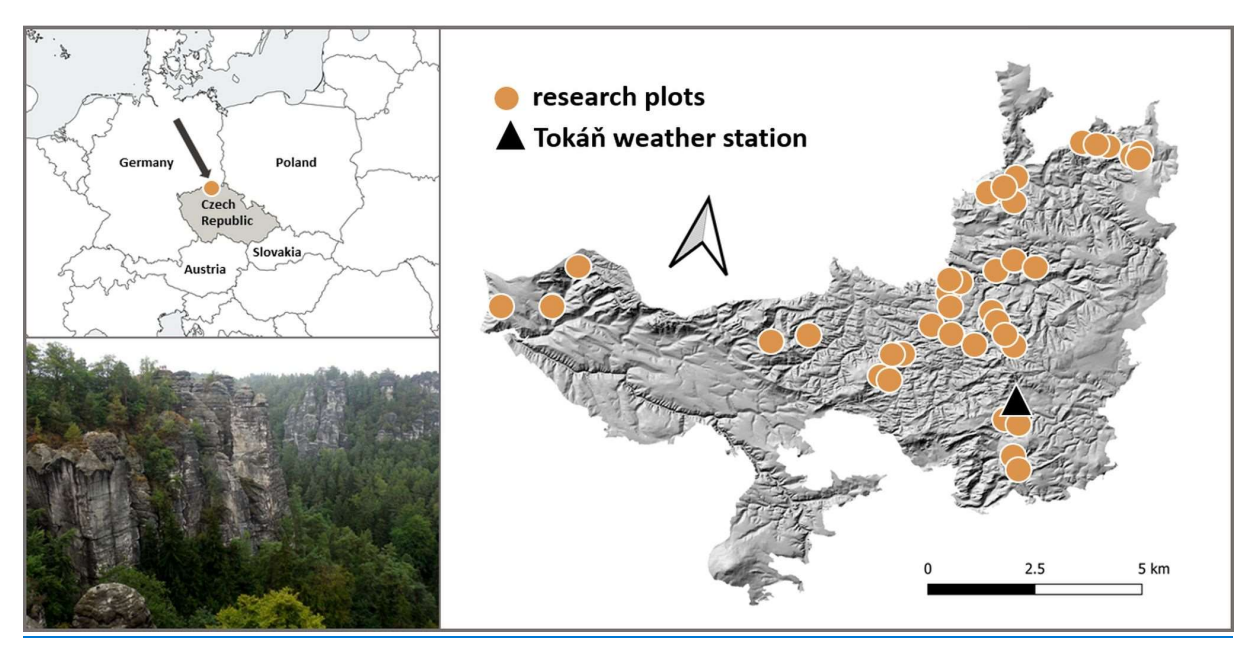


Figure 1: We measured microclimate and simultaneously recorded bryophyte species composition at 38 permanent research plots within the Bohemian Switzerland National Park in Central Europe—(a). This forested area has rugged terrain creating steep environmental gradients over short distances—(b). The location of the 38 research plots and the Tokáň weather station within the area of the national park (e).

Most of the Bohemian Switzerland is covered with coniferous forests. Historically planted Norway spruce (*Picea abies*) planted mostly during the 19<sup>th</sup> and 20<sup>th</sup> century predominates in the valleys and on the plateaus, while patches of semi-natural forests are dominated either by Scots pine (*Pinus sylvestris*) on the upper slopes and rocky ridges or by European beech (*Fagus sylvatica*) on more mesic sites.

The nutrient-poor and strongly acidic soils result in a relatively low diversity of vascular plants, which contrasts with the <u>exceptionally</u> rich bryophyte flora (Härtel et al., 2007). <u>The Bohemian Switzerland currently hosts With</u> more than 300 bryophyte species, the <u>Bohemian Switzerland is and therefore represents</u> a hotspot of bryophyte diversity in Central Europe (Marková, 2008).

The bryophyte flora of the Bohemian Switzerland is dominated by <u>forest</u> species like *Tetraphis pellucida*, *Bazzania trilobata*, and *Dicranum scoparium*. These dominant floristic elements are enriched by <u>azonal disjunct</u> occurrences of (sub)alpine or (sub)montane (e.g., *Hygrobiella laxifolia*, *Geocalyx graveolens*, *Anastrophyllum michauxii*), boreal (e.g., *Dicranum majus*, *Rhytidiadelphus subpinnatus*)<sub>2</sub> and (sub)oceanic (e.g., *Tetrodontium brownianum*, *Plagiothecium undulatum*) species (Härtel et al., 2007; Marková, 2008).

#### 2.2 Field data collection

We recorded bryophyte species composition and measured microclimate on 38 permanent plots within the Bohemian Switzerland National Park (Fig. 1). These plots were selected through stratified-random sampling to capture the main microclimatic gradients within the core zone of the national park. Specifically, using GIS and LiDAR-based digital terrain model, we first divided the study area into geographical strata defined by the terrain (valley bottoms, lower slopes, upper slopes, and ridges) and further separated the slopes with predominantly northern and southern orientation. Within each stratum, we randomly selected an equal number of locations separated by at least 50 m. In the field, we navigated to the selected location with GPS device and placed the center of plot 1.5 m to the north from the nearest tree.

- Within each permanent plot, we installed HOBO U23 ProV2 (Onset, USA) microclimatic datalogger protected by
- a white radiation shield with good ventilation and placed at 1.5 m height on the north side of a tree nearest to
- the plot center. Each HOBO datalogger was protected by a white radiation shield with good ventilation
- and -measured air temperature (resolution 0.02 °C, accuracy ± 0.21 °C) and relative humidity (resolution 0.05 %,
- accuracy  $\pm 2.5$  %) every 30 minutes from 1 June to 31 August 2022.
- 140 Simultaneously with microclimate measurements, we recorded the presence of all bryophyte species in each
- research plot following the nomenclature of the Czech national checklist (Kučera et al., 2012). We deliberately
- sampled bryophytes in a relatively small <u>circular plot with 1 m radius area-(3.14 m²)</u> without any exposed rocks
- or big stones to reduce the possible effects of within-plot environmental heterogeneity (Rambo and Muir, 1998;
- 144 Vanderpoorten and Engels, 2002; Schmalholz and Hylander, 2011).

#### 2.3 Microclimate data processing

- First, we checked the microclimatic time series using visually inspection and then with standard automated
- procedures implemented in the myClim R package (Man et al., 2023). Air humidity measurement with
- microclimatic loggers is sensitive to water condensation, resulting in unrealistically high measurements for prolong
- periods of time (Ashcroft and Gollan, 2013; Feld et al., 2013). We therefore carefully checked microclimatic time
- series and found no signs of the condensation effect.
- Using checked air temperature and relative humidity data, we first calculated the saturated vapor pressure (Psat)
- following the updated Buck formula (Buck, 1981, 1996):
- $P_{sat} = (1.003 + 4.18 \times 10^{-6} \times 101 \ kPa) \times 0.61115 \times e^{((23.036 /333.7)*(t/(279.82 + t)))},$
- where *t* is air temperature [ $^{\circ}$ C].
- Then, we calculated the actual vapor pressure (Pair) using the Tetens's formula (Tetens, 1930):
- 156  $P_{air} = P_{sat} \times \left(\frac{rh}{100}\right)$ ,

- where rh is relative humidity [%].
- Finally, we calculated atmospheric VPD as the difference between P<sub>sat</sub> and P<sub>air</sub> (Jones, 2014).
- 159 <u>Using the resulting microclimatic time series, we calculated three variables representing evaporative stress</u>
- 160 (Tab. 1). First, we calculated the average daily maximum temperature (T<sub>max</sub>). While T<sub>max</sub> is ecologically less
- meaningful proxy for evaporative stress than atmospheric VPD (Campbell and Norman, 1998; Eamus et al., 2013),
- several previous studies identified T<sub>max</sub> as highly relevant microclimatic variable linked to evaporative stress
- and affecting species composition and richness of forest vascular plants and bryophytes within the central Europe
- 164 (Macek et al., 2019, Man et al., 2022). Then, we calculated two variables capturing different aspects of VPD driven
- evaporative stress. First, we calculated the average daily maximum VPD (VPD<sub>max</sub>), which represents site-specific
- microclimatic extremes (Ashcroft and Gollan, 2013). Second, we calculated the average daily mean VPD, which
- represents time-aggregated evaporative demand experienced by bryophytes on each site.
- 168 To disentangle the drivers of spatio-temporal VPD variability over the landscapeFrom the resulting time series,
- we extracted calculated also plot-specific daily average values of maximum VPD and Psat and Pair values at the
- 170 time of daily maximum VPD (Tab. 1).
- 171 Table 1: Overview of microclimatic variables representing evaporative stress (T<sub>max</sub>, VPD<sub>max</sub>, VPD<sub>mean</sub>) and its
- 172 components (P<sub>sat.</sub> P<sub>air</sub>). For each variable, we provide the overall mean and range of plot-specific averaged daily values
- measured continually during summer 2022 on 38 forest research plots in the Bohemian Switzerland National Park,
  Czech Republic. Summary statistics of microclimatic variables measured in 38 forest research plots during summer

(June August 2022). Vapor pressure deficit is the average daily maximum, while saturated and actual vapor pressure are averages of these variables at the time of maximum daily VPD.

-	Abbreviation	Mean across a	all plots Ran	ge of plot means	
Saturated vapor pressure	$P_{\text{sat}}$	4.00 kPa	<del>2.61 5.02 kPa</del>		
Actual vapor pressure	$\mathbf{P}_{\mathbf{air}}$	<del>1.90 kPa</del>	1.75 2.08 kPa		
Vapor pressure deficit	<del>VPD</del>	2.09 kPa	<del>0.62 3.17 kPa</del>		
Microclimatic variable		Abbreviation	Overall mean	Range of plot means	
Maximum air temperature		$T_{\text{max}}$	24.26 °C	18.80–27.64°C	
Maximum vapor pressure defic	it	$VPD_{max}$	2.09 kPa	0.62–3.17 kPa	
Mean vapor pressure deficit		$VPD_{mean}$	0.85 kPa	0.23–1.16 kPa	
Mean saturated vapor pressure		$\mathbf{P}_{\text{sat}}$	2.63 kPa	2.09–2.93 kPa	
Mean actual vapor pressure		$P_{air}$	1.78 kPa	1.66–1.90 kPa	

#### 2.4 Data analysis

175

176

177

178

179

180181

182

183

184

185

186

187

188

189

190

191

192

193

194

195

196

197

198

199

200

#### 2.4.21 Bryophyte community composition, richness and structureies

In our analysis, we focused on explored the relationship between microclimatic variables representing evaporative stress atmospheric VPD and bryophyte community composition, structure, and richnesscommunities through three steps. First, we identified explored the VPD, Psat, and Pair air relationship to the main gradients in community composition and explored their relationship with variables representing evaporative stress, we quantified the VPD link to species richness. Then, to explore which variable representing evaporative stress is more closely associated with bryophyte community composition and richness, we calculated the variability in directly tested VPD ) effects on species composition and richness explained by the mean and maximum atmospheric VPD and maximum air temperature. Further, to disentangle the effects of atmospheric VPD from the effects of the maximum temperature, we partition the explained variability into independent and shared fractions. Finally, we directly tested the link between VPD effects on species composition and bryophyte community structure through nestedness analysis. To explore the main gradients in the bryophyte community composition, we used non-metric multidimensional scaling (NMDS) to extract the main patterns in bryophyte community composition expressed with based on the Sørensen dissimilarity index. We calculated two-dimensional NMDS with the weak treatment of ties, a maximum of 500 random starts, and 999 iterations in each NMDS run using metaMDS function from the vegan R package version 2.6-4 (Oksanen et al., 2022). To maximize variance along the first ordination axis, we centered and rotated the resulting two-dimensional configuration with principal component analysis. To explore whether how main compositional gradients correlate with microclimate variables representing evaporative stress, we passively projected gradients invectors of maximum and mean VPD, Psatz and Pair and maximum temperature into the NMDS ordination space and tested the significance of the fit with 999 random permutations using the envfit function from vegan R package (Oksanen et al., 2022). Finally, we projected bryophyte species richness gradients into the NMDS ordination space using a generalized additive model fitted through *ordisurf* function from *vegan* R package (Oksanen et al., 2022).

201 To quantify the relationship between the microclimatic variables representing evaporative stress VPD and species 202 richness expressed as a number of bryophyte species recorded in the plot, we used a generalized additive model 203 (GAM) fitted with the R package mgcv 1.9.1 (Wood, 2011). We used GAM with Poisson distribution, log link 204 function, and smooth terms fitted by thin plate regression splines without null space penalization and smoothing 205 parameter estimation using restricted maximum likelihood. To assess the statistical significance, we used a  $\chi^2$  test 206 comparing the fitted model to the only intercept null model. 207 To calculate the proportion of variability in bryophyte community composition explained by microclimatic 208 variables representing evaporative stress, we used distance-based RDA (McArdle and Anderson, 2001) calculated 209 on the same Sørensen dissimilarity matrix as used for NMDS. We calculated the distance-based RDA (db-RDA) 210 with dbrda function from vegan R package (Oksanen et al., 2022) and assess the statistical significance using 999 211 random permutations of the raw data (Legendre et al., 2011). 212 As all three microclimatic variables representing evaporative stress were correlated (Appendix A), we explored 213 their shared and independent effects on bryophyte community composition and richness through variation 214 partitioning (Legendre, 2008). Because VPD<sub>max</sub> and T<sub>max</sub> were almost identical (Pearson R = 0.98), we disentangled shared and independent effects of substantially less correlated  $\underline{VPD}_{mean}$  and  $\underline{T}_{max}$  (Pearson R = 0.78). 215 To quantify their independent and shared effects, we partitioned the variation in bryophyte community 216 217 composition explained by atmospheric VPD<sub>mean</sub> and T<sub>max</sub> using adjusted R<sup>2</sup> (Peres-Neto et al., 2006) calculated 218 with the varpart function from the vegan R package (Oksanen et al., 2022). 219 To quantify the shared and independent effects of atmospheric VPD<sub>mean</sub> and T<sub>max</sub> on species richness, we 220 partitioned the deviance explained in GAM models. First, we related species richness to atmospheric VPD<sub>mean</sub> and 221 T<sub>max</sub> in the full GAM, when both variables were used simultaneously as predictors. Then, we fitted two partial 222  $\underline{GAMs \ (first \ with \ \underline{VPD}_{mean}, \ second \ with \ \underline{T_{max}} \ as \ explanatory \ variable \underline{s}). \ To \ prevent \ different \ smoothing \ parameters}$ 223 in the partial models, we extracted smoothing parameters from the full GAM and used them in both partial GAMs 224 (Hjort et al., 2012). To assess the statistical significance, we compared each model against the null model with 225 only intercept using a  $\chi^2$  test. To assesses the significance of the independent effects of atmospheric VPD and  $T_{max}$ , 226 we compared partial GAMs with the full GAM using  $\chi^2$  test. 227 Finally, we used nestedness analyses (Ulrich et al., 2009) to test the VPD effects on bryophyte community 228 structure. To directly test the two hypotheses about the bryophyte community structure along the VPD gradient, 229 we first order the community matrix along the gradient of increasing plot-specific VPD<sub>mean</sub>. To test the first 230 hypothesis that the bryophyte communities from sites with high VPD are nested subsets of bryophyte communities 231 from sites with low VPD, we used NODF<sub>sites</sub> metric (Almeida-Neto et al., 2008). To test the second hypothesis 232 that more frequent bryophyte species occur along the whole VPD gradient, but less frequent species are 233 concentrated on sites with low VPD, we used NODF<sub>species</sub> metric (Almeida-Neto et al., 2008). To calculate both 234 NODF metrics, we used nestednodf function from the vegan R package (Oksanen et al., 2022). 235 We used a null model approach to assess the statistical significance of nestedness patterns (Ulrich et al., 2009). 236 Specifically, we compared the observed NODF values to the distribution of 999 NODF values calculated through 237 the conservative R1 null model, which maintains species richness of the site and uses species frequencies as probabilities of selecting species (Wright et al., 1997). To quantify the difference between the observed NODF 238 239 values and the NODF values generated by the R1 null model, we calculated the standardized effect size (SES) 240 expressing the number of standard deviations that the observed NODF value differs from the mean NODF value

- of the simulated assemblages (Ulrich et al., 2009). To construct the null models and to calculate SES, we used the
- 242 <u>oecosimu</u> function from the vegan R package (Oksanen et al., 2022).
- We used R version 4.4.0 (R Core Team, 2024) for complete data analysis and figure preparation. For the
- 244 color-blind safe gradients scheme of Fig. 2 and Fig. 45, we used the R package scico 1.5.0 (Pedersen and Crameri,
- 245 2023).

246

#### 2.4.1-2 Spatial VPD variability across the landscape

- 247 <u>Using the time-series of both VPD components (P<sub>sat</sub> and P<sub>air</sub>), we explored their spatio-temporal variability</u>
- and quantify their influence on the VPD variability over the landscape. First, we explored how variable was VPD
- 249 and both its components over the landscape in a daily timesteps. Then, we averaged this daily variability into
- 250 the overall measure of spatial variability in VPD, Psat, and Pair during the whole study period. Finally, we used
- variation partitioning to quantify how much was VPD variability controlled by P<sub>sat</sub> and P<sub>air</sub>.
- To quantify spatial variability in daily VPD and both its components; (Psat and Pair) over the landscape, we
- calculated the standard deviation (SD) of the plot-specific daily maximum mean VPD, and corresponding Psat and
- Pair values among all study plots. In this first step, we calculated SD of these microclimatic variables for every day
- within the study period separately. -and-Then we averaged these daily inter-plot SD values separately for VPD,
- 256 P<sub>sat</sub> and P<sub>air</sub> into over the study period as an overall measure of spatial variability for each microclimatic variable
- 257 <u>during the whole study period</u>.
- 258 Finally, tTo disentangle the contribution of P<sub>sat</sub> and P<sub>air</sub> to the VPD variability over the landscape, we performed
- variation partitioning (Legendre, 2008) based on a multiple linear regression model and adjusted R<sup>2</sup> (Legendre,
- 260 2008) with the plot-specific average daily maximum mean VPD as the response variable and the average daily
- 261 values mean of P<sub>sat</sub> and P<sub>air</sub> at the time of daily maximum VPD as the predictors.

#### 3. Results

262

263

#### 3.2-1 Bryophyte community composition, richness and structureies

- 264 In total, we recorded 39 bryophyte species: 14 liverworts and 25 mosses (Appendix C, Tab. C1). The species
- 265 richness was highly variable among the plots while the average number of species per plot was 8, the minimum
- 266 <u>was 1</u> and the maximum 21. The most frequent species were Dicranum scoparium (n = 32), Leucobryum
- juniperoideum (n = 26) and Hypnum cupressiforme (n = 24).
- 268 Main patterns in community composition and species richness reflected the gradient of evaporative stress (Fig. 2).
- 269 Gradients in atmospheric VPD and P<sub>sat</sub> were the most closely related to the main patterns in community
- 270 composition (vegan::envfit VPD<sub>mean</sub>:  $R^2 = 0.52$ , p = 0.001;  $VPD_{max}$ :  $R^2 = 0.37$ , p = 0.001,  $P_{sat}$ :  $R^2 = 0.52$ ,
- 271 p = 0.001). Gradient in  $T_{\text{max}}$  was highly correlated to the gradients in VPD (Fig. 2), but main patterns in community
- composition were less related to  $T_{\text{max}}$  than to VPD (vegan::envfit  $T_{\text{max}}$ :  $R^2 = 0.32$ , p = 0.003; vegan::envfit –
- VPD<sub>mean</sub>:  $R^2 = 0.52$ , p = 0.001;  $VPD_{max}$ :  $R^2 = 0.37$ , p = 0.001,  $P_{sat}$ :  $R^2 = 0.52$ , p = 0.001). Finally, gradient in  $P_{air}$
- 274 was also significantly related to the main patterns in community composition, but its effect was lower and largely
- independent from other microclimatic variables (vegan::envfit  $-P_{air}$ :  $R^2 = 0.26$ , p = 0.008).
- 276 The number of bryophyte species was higher in plots with low VPD and declined with an increasing VPD (Fig. 2).
- 277 Both atmospheric VPD and maximum temperature were significantly associated with species richness, but

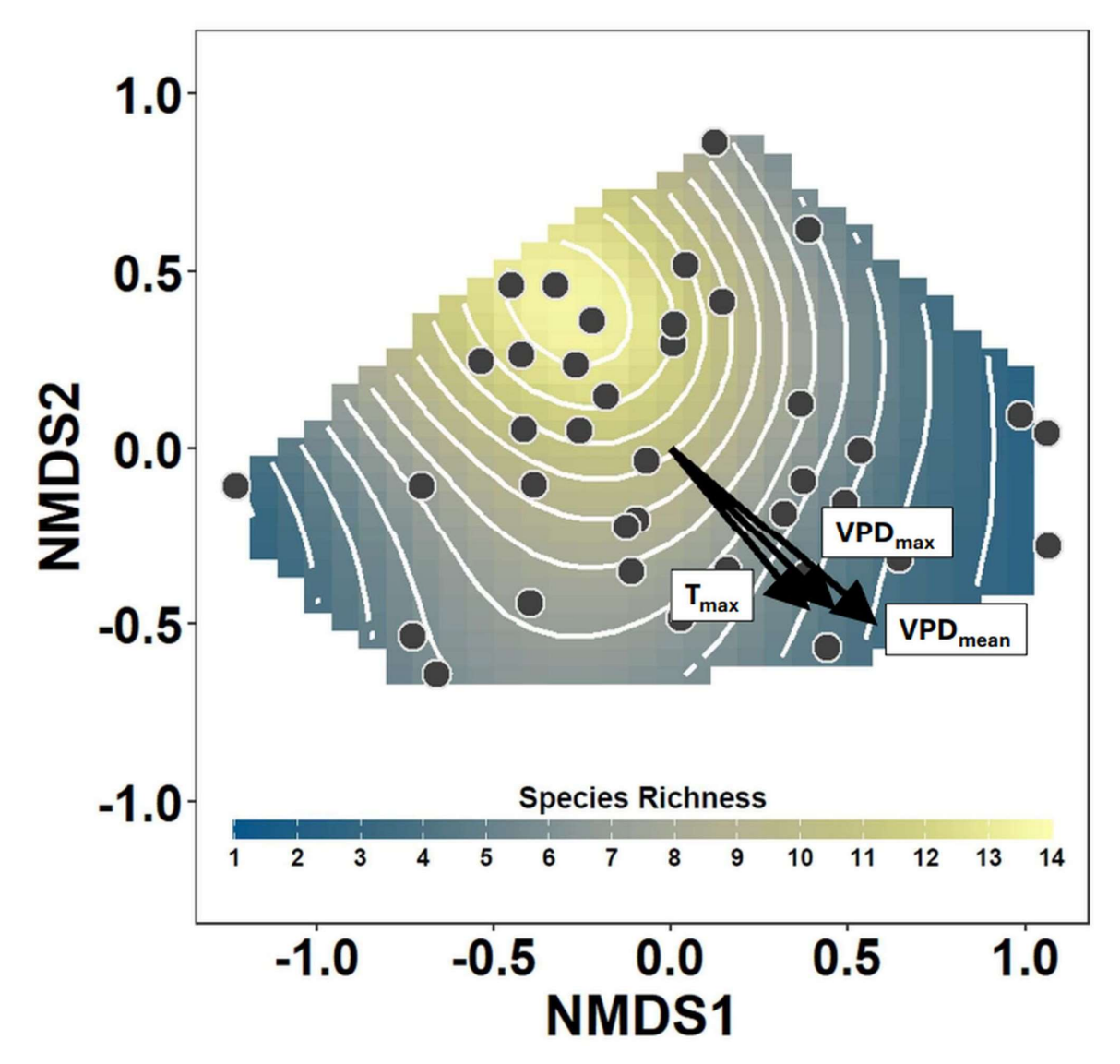


Figure 42: Nonmetric multidimensional scaling (NMDS) of the bryophyte community composition showing main gradients in bryophyte assemblages sampled at 38 temperate forest plots. Points show the positions of the individual plots within the NMDS ordination space, and the vectors show the gradients in the average maximum air temperature (Tmax), maximum VPD (VPDmax) and mean VPD (VPDmeant). The smooth surface and associated contours fitted into the NMDS ordination space with a generalized additive model show the pattern of decreasing species richness with increasing atmospheric evaporative stress demand (number of species per plot) fitted into the NMDS ordination space with a generalized additive model.

The mean VPD explained substantially more variation in species composition than the maximum VPD and the maximum temperature (Table 2). When used independently, both  $\overline{VPD}_{mean}$  and  $\overline{T}_{max}$  were significant predictors of bryophyte community composition (Table 2). However, the effect of  $\overline{T}_{max}$  almost completely overlaps with  $\overline{VPD}_{mean}$  (Fig. 3). When we controlled for the effect of mean VPD, maximum temperature did not explain significant part of variation in community composition (*vegan::dbrda* – adj.  $R^2 = 0$  %, p = 0.764) or in species richness ( $mgcv::gam - D^2 = 3.72$  %, p = 0.174). In contrast, the mean VPD explained a significant part of variation in species composition and richness even after the controlling for maximum temperature

(vegan::dbrda – adj.  $R^2 = 6$  %, p = 0.003), see Fig. 3. Therefore, the mean VPD explained substantially more variation in bryophyte community composition and richness than maximum temperature and maximum temperature did not have any significant effects independent from the mean atmospheric VPD (Fig. 3).

Atmospheric VPD was a significant predictor of the community composition of forest bryophytes. The average daily maximum VPD explained 10.95 % of the variation in species composition expressed with the Sørensen index ( $\frac{1}{2}$  pseudo  $\frac{1}{2}$  = 4.43,  $\frac{1}{2}$  = 0.001) and  $\frac{1}{2}$  = 0.001 and  $\frac{1}{2$ 

index (: pseudo F = 5.63, p = 0.004).

Table 2: Variation in community composition and species richness explained by three microclimatic variables representing evaporative stress. To quantify variation explained by each variable, we used distance-based RDA (db-RDA) for community composition and generalized additive models (GAM) for species richness.

	<b>Community composition (db-RDA)</b>			Species richness (GAM)		
	Variation (R <sup>2</sup> )	pseudo-F	p-value	Deviance (D <sup>2</sup> )	<u>χ2</u>	<u>p-value</u>
Microclimatic variable						
mean VPD	<u>16.09 %</u>	<u>6.90</u>	0.001	<u>32.8 %</u>	<u>27.04</u>	< 0.001
maximum VPD	<u>10.95 %</u>	4.43	0.001	<u>31.2 %</u>	23.37	< 0.001
maximum T <sub>air</sub>	<u>9.21 %</u>	3.65	0.003	14.0 %	11.13	0.007

# species composition species richness

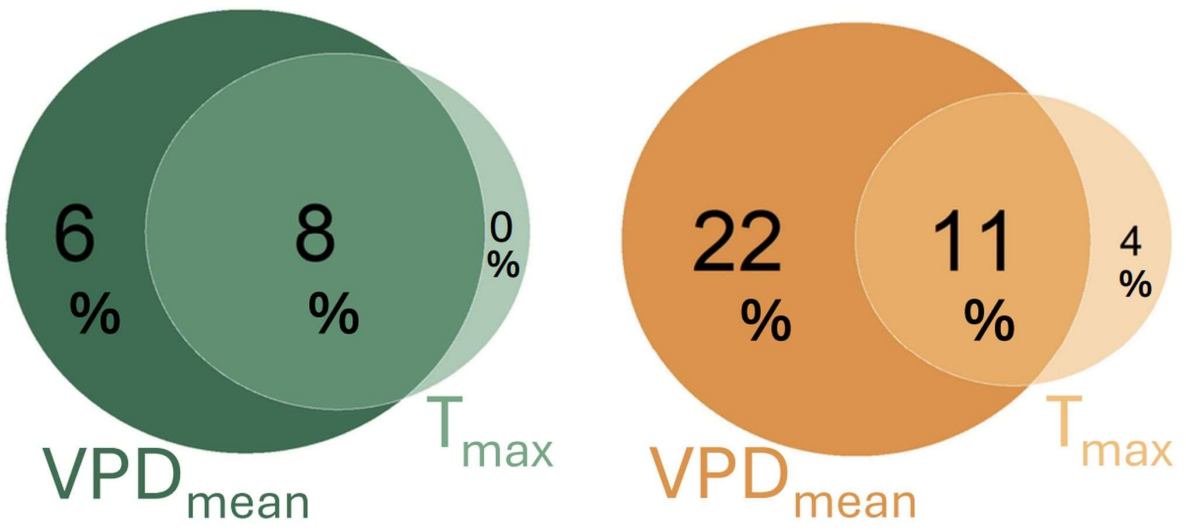


Figure 3: Variation partitioning showing independent and shared effect of mean VPD (VPD<sub>mean</sub>) and maximum air temperature ( $T_{max}$ ) on bryophytes species composition and richness in 38 forest plots. Values represent adjusted  $R^2$  from db-RDA for species composition and explained deviance from GAM for species richness. While VPD<sub>mean</sub> has significant effects even after the controlling for  $T_{max}$  both for species composition (p = 0.003) and richness (p = < 0.001), the unique effects  $T_{max}$  was non-significant both for species composition (p = 0.764) and richness (p = 0.174).

Bryophyte community structure was closely related to the gradient of mean atmospheric VPD (Fig. 4). Bryophyte communities from plots with higher VPD were generally impoverished and compositionally nested subset of the communities from sites with lower VPD ( $vegan::oecosimu - NODF_{sites} = 39.17$ , SES = 4.26, p = 0.001). Moreover, while frequent species occurred along the whole VPD gradient, rare species occurred preferably on sites with low VPD ( $vegan::oecosimu - NODF_{species} = 29.97$ , SES = 3.34, p = 0.003).

At the species level, small liverworts (e.g. Riccardia multifida, Lophozia ventricosa) and hygrophilous bryophytes (e.g. Polytrichum commune, Bazzania trilobata), as well as species with boreal (e.g. Dicranum majus) and (sub)oceanic (e.g. Mylia taylorii, Plagiothecium undulatum) distributionspecies preferred plots with low atmospheric VPD (Fig. 4). In contrast, regionally frequent species like Hypnum cupressiforme, Polytrichum formosum or Dicranum scoparium occurred also in plots with higher atmospheric VPD (Fig. 4).

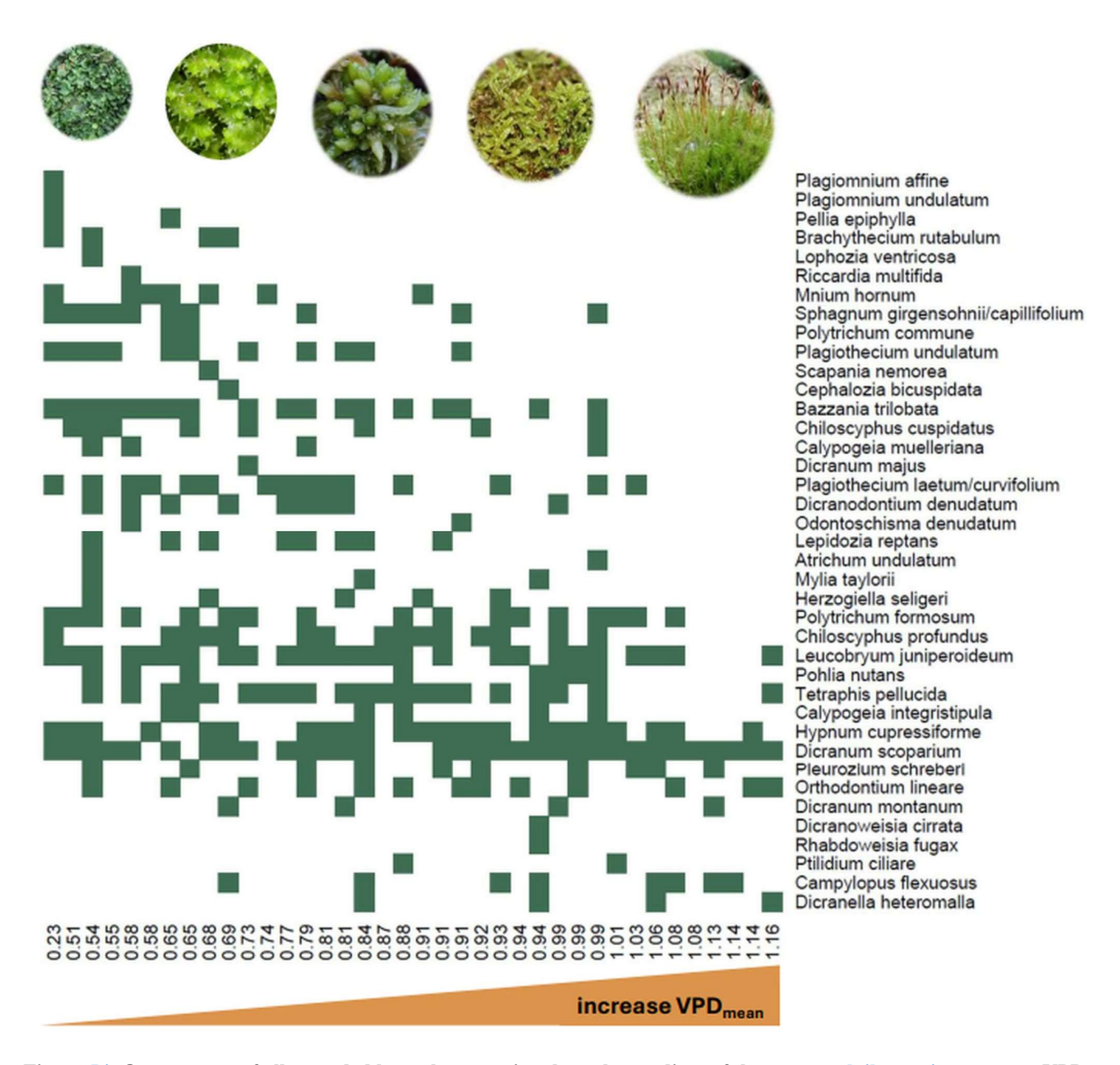


Figure 54: Occurrences of all recorded bryophyte species along the gradient of the average daily maximum mean VPD measured at 38 forest plots. Plots are sorted from the lowest to highest mean VPD and each filled square shows the presence of the focal species within the plot. While rare and azonally occurring species near their distributional range limits prefer sites with low VPD, mesic forest species occur along the whole VPD gradient.

#### 3.1-2 VPD variability across the landscape

VPD in the forest understory was highly variable across the landscape; (Fig. 25). While the variability in saturated vapor pressure was comparable to the variability in VPD, actual vapor pressure was much less variable among the sites (Fig. 25). In average, tThe landscape-scale spatial variability of  $P_{sat}$  (average daily SD = 0.550.20 kPa) was almost four three times higher than the spatial variability of  $P_{air}(SD = 0.140.07 \text{ kPa})$ .

The VPD values measured every 30 minutes during summer months ranged from 0 kPa to 8.83 kPa with an overall mean of 0.85 kPa. The overall average daily maximum VPD was 2.09 kPa and ranged from 0.62 to 3.17 kPa among the plots (Tab. 1 and Appendix A, Fig. A1 a Fig. A2).

### Spatial variation in

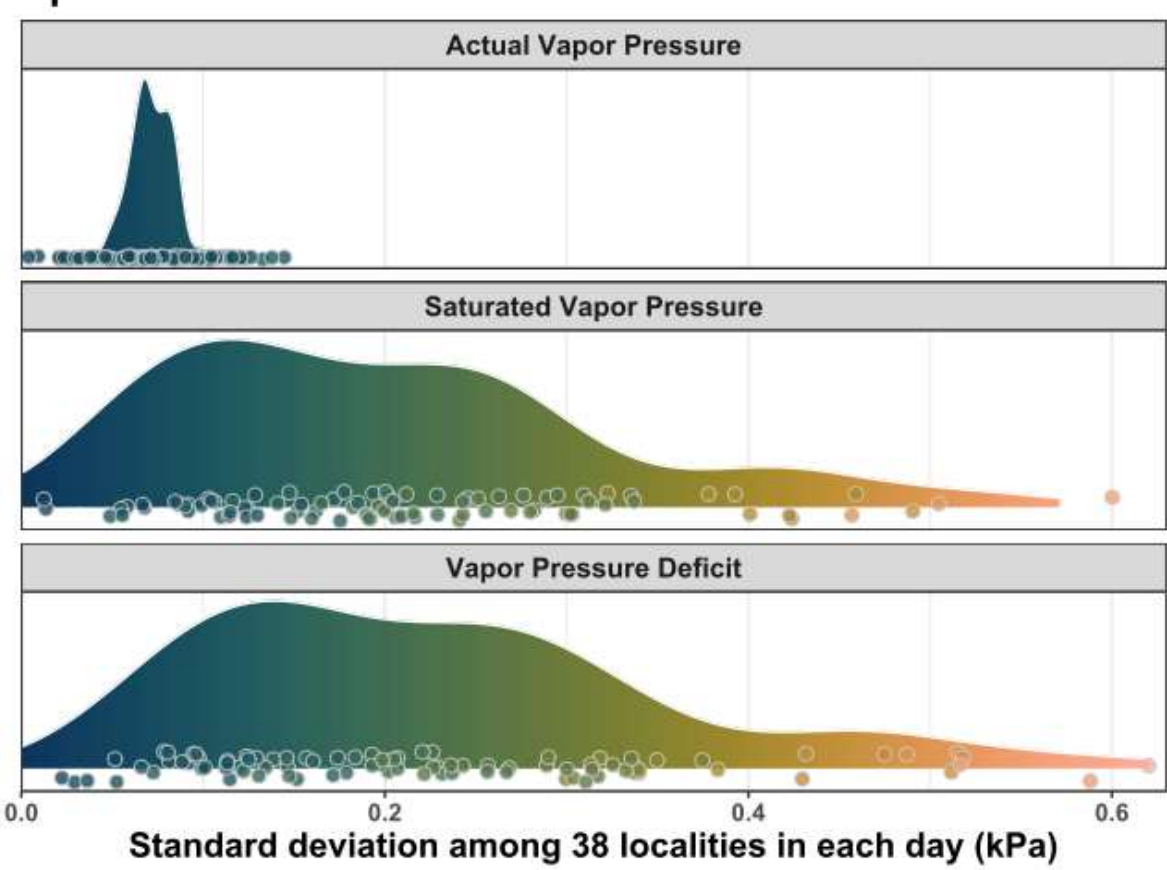


Figure 25: Spatio-temporalal variability of VPD and its components – saturated and actual atmospheric vapor pressures. Each data point shows the standard deviation of the plot-specific daily mean values simultaneously measured at 38 forest plots, and density plots summarize this spatio-temporalal variability over the summer season. The individual data points were slightly jittered for better visibility.

Saturated vapor pressure was also Tthe dominant driver of VPD variability across the landscape was temperature-driven saturated vapor pressure (Fig. 36). because In a univariate linear regression model,  $P_{sat}$  explained 97-93 % of VPD variability, while  $P_{air}$  explained only 3-30 %. However,  $P_{sat}$  and  $P_{air}$  were negatively correlated (Pearson R = -0.31) and variation partitioning based on multiple regression model showed that the  $P_{air}$  uniquely explained only 7 % of variability in VPD (Fig. 6). Therefore, temperature-driven  $P_{sat}$  was the dominant driver of VPD variability, while spatial variation in  $P_{air}$  contributed surprisingly little to the overall VPD variability across the landscape.

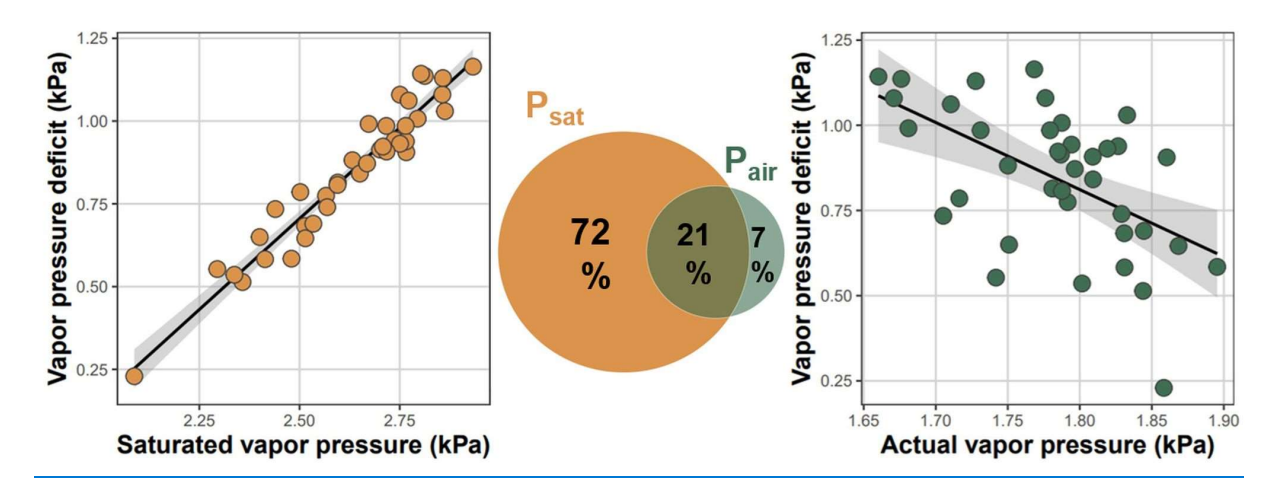


Figure 36: Atmospheric vapor pressure deficit (VPD) at 38 forest plots sampled over topographically diverse landscape was driven by temperature-dependent saturated vapor pressure (b), while actual vapor pressure was weakly not related to local VPD (a). Each dot represents the average daily maximum mean VPD and the corresponding average mean saturated and actual vapor pressure measured during the summer—season\_at 38 forest plots established over topographically diverse landscape. Venn diagram shows variation (adjusted R<sup>2</sup>) in mean VPD explained solely by mean saturated (P<sub>sat</sub>) and mean actual (P<sub>air</sub>) vapor pressure and the variation explained jointly by both predictors.

#### 4. Discussion

347

348

349 350

351

352

353

354

355

356

357

358

359

360

361

362

363

364

365

366367

368

369

370

371

372

373

374

375

376

377

We found that community composition and richness of forest bryophytes was significantly affected by atmospheric VPD. Our findings have important implications both for theoretical and applied ecology. First, the variation in VPD over the landscape was <u>largely</u> controlled by <u>maximum</u> air temperature. Therefore, these two microelimatic variables air temperature and VPD are tightly coupled at biologically relevant scales, and their effects are hard to disentangle with observational data. Interestingly, this coupling was strongest between maximum VPD and maximum temperature and Mmaximum temperatures were was previously identified as a key driver of bryophyte and vascular plant species distribution in temperate forests (Macek et al., 2019; Man et al., 2022). Unfortunately, these studies did not measure VPD. Considering our results, the importance of maximum temperature does not necessarily stem from its direct effects on plant ecophysiology, but more likely from strong temperature control of VPD variability over the landscape. Nevertheless, this new hypothesis needs further testing. Interestingly, we also found that mean VPD was a much better predictor of bryophyte community composition and richness than maximum VPD or maximum temperature. At the same time, maximum temperature did not explain any additional variation in species composition and richness not explained by mean VPD. Our results thus provide strong evidence that the mean VPD is more relevant predictor of bryophyte community composition and richness than maximum temperature or maximum VPD. The unique effects of mean VPD, not reflected by the maximum temperature or maximum VPD, suggest that bryophyte communities are more sensitive to the long-term characteristics of site microclimatic conditions, rather than to short-term microclimatic extremes captured by maxima. Second, our results showing that actual vapor pressure is relatively constant across the landscape imply that it is possible to estimate VPD from local microclimate air temperature measurements combined with non-local measurements of air relative humidity, for example from a nearby weather station. While the general applicability of this approach should be further tested across spatial scales (Dahlberg et al., 2020), in various environmental settings and across different vegetation types, our findings suggest that local VPD can be reasonably estimated

(Appendix B, Fig. B1). This finding thus opens exciting possibilities for further research as local temperature measurements are increasingly available all over the world (Lembrechts et al., 2020). However, it should be stressed that this approach generates VPD estimates which provide reasonable ranking of the sites along the VPD gradient, but generally overestimate the VPD (Appendix B, Fig. B1), likely because it does not account for locally higher actual vapor pressure, for example near springs, water bodies or on permanently waterlogged soils.

#### 4.1 VPD variability across the landscape

383

384

385

386

387

388

389

390

391

392

393

394 395

396

397

398

399

400

401

402

403

404

405

406

407

408 409

410

411

412

413

414

415

VPD variability at finer scales (Wörlen et al., 1999).

Large spatial variability in atmospheric VPD structured forest bryophyte communities across the landscape. Interestingly, VPD variation was driven by temperature-controlled P<sub>sat</sub>, while P<sub>aer</sub>-P<sub>air</sub> was relatively constant across the landscape. This finding is important, as the actual vapor pressure should also be variable across the landscape (Ogeé et al. 2024; Johnston et al., 2025). However, our findings suggest that the local and spatially highly heterogeneous processes like evaporation from soil and water surfaces and plant transpiration do not contribute much-little to the landscape-scale variation in VPD, even in the topographically diverse landscape with steep microclimatic gradients. While maximum VPD was solely driven by saturated vapor pressure and therefore maximum temperature, the mean VPD was more affected by actual vapor pressure. However, saturated and actual vapor pressures were negatively correlated and therefore the unique effect of actual vapor pressure on spatial pattern in atmospheric VPD was surprisingly small. The landscape-scale variation in atmospheric VPD was therefore controlled by microclimate temperature variation. Microclimate temperature variation over the landscape, crucial for community ecology, is largely dictated by land-surface topography (Dobrowski, 2011). Land-surface topography controls also maximum air temperatures in the forest understory (Vanwalleghem and Meentemeyer, 2009; Macek et al., 2019) and therefore spatial variability in saturation vapor pressure. However, we were surprised that the highly localized processes like evapotranspiration did not contribute much to the spatial variability in absolute air humidity despite our study area with extremely rugged topography and contrasting forest vegetation types. Therefore, spatial variability in absolute air humidity seems to be determined mostly by processes operating at much larger scales like atmospheric circulation and precipitation patterns (Campbell and Norman, 1998). Nevertheless, local topographic depression with waterlogged soils and especially the proximity to flowing water or permanent water bodies can locally elevate actual vapor pressure and therefore decrease atmospheric VPD (Wei et al. 2018, Ogeé et al. 2024). However, our results suggest that the overall pattern in atmospheric VPD will generally follow changes in air temperature and therefore future climate warming will result in non-linear increase in evaporative stress across the landscapes. Given the growing recognition of VPD importance for many ecosystem processes, plant distribution, and community assembly (Grossiord et al., 2020; Kopecký et al., 2024; Novick et al., 2024), the approach we developed here to disentangle the contribution of saturated versus actual vapor pressure can provide new insights into the drivers of VPD variability across spatial and temporal scales. So far, the knowledge of the relative importance of saturated versus actual vapor pressure is limited, therefore it is difficult to compare our results with other studies. Nevertheless, a comparison of the drivers of VPD variability across agricultural fields in Germany supports our conclusion that temperature-driven variability in saturated vapor pressure is a dominant control of

#### 4.2 VPD effects on bryophytes

416

417

418

419

420

421

422

423

424

425

426

427428

429

430

431

432

433

434435

436

437

438

439

440

441

442

443

444

445

446

447

448

449

450

451

452

453

Bryophytes inevitably lose water when exposed to the air with non-zero VPD (Hinshiri and Proctor, 1971; Busby and Whitfield, 1978). In contrast to vascular plants, bryophytes tolerate desiccation and become metabolically inactive in the absence of water (Proctor, 2000). When conditions improve, bryophytes quickly reactivate physiological processes such as respiration, photosynthesis, cell cycle, or normal cytoskeleton function (Proctor, Ligrone, et al., 2007; Proctor, Oliver, et al., 2007). However, this reactivation requires a lot of energy, for example to produce specific repair proteins (Oliver and Bewley, 1984; Zeng et al., 2002) or to maintain the integrity and normal function of cell organelles and membranes (Platt et al., 1994). Prolonged periods without evaporative stress are therefore key for bryophyte growth and long-term survival (Proctor, Oliver, et al., 2007; Merinero et al., 2020). At full turgor, Bbryophyte cells at full turgor have osmotic potential rarely more negative than -2 MPa (Proctor, 2000). An osmotic potential of -1.36 MPa is in equilibrium with air at 20 °C and 99% relative humidity (i.e. VPD < 0.03 kPa). If the temperature remains at 20 °C, but the relative humidity drops to 90 %, the water potential outside the bryophyte body decreases to -14 MPa (Proctor, 2000) and bryophytes start to lose water. To maintain full turgor and normal cell function, bryophytes thus need free liquid water close to the cells. However, this external water completely evaporates within 45-50 minutes if atmospheric VPD reaches 1.22 kPa (León-Vargas et al., 2006). Once the external water evaporates, bryophyte cells rapidly lose turgor, metabolic activity slows down, and carbon fixation decreases. In our study region, microclimatic such favorable conditions without evaporative stress and with VPD lower than 0.03 kPa and therefore without evaporative stress for bryophytes (Proctor, 2000) occurred on average only 9 % of the measurement time. However, there was large variability among the sites, resulting in Large VPD variability over the landscape creates fine-scaled landscape mosaic of sites with widely different evaporative stress. We found that this fine-scale VPD variation -and this environmental template structured bryophyte communities. Regionally rare species with disjunct distribution in central Europe generally preferred sites with low VPD. These species – otherwise typical for (sub)montane, boreal, or (sub)oceanic regions – are approaching their distributional limits within our study area (Hill and Preston, 1998). For these species, sites with low VPD serve as microclimatic refugia within an otherwise unsuitable landscape matrix. In contrast, regionally widespread mesic bryophytes occurred along the whole VPD gradient. Fine-scale variation in VPD thus functions as an environmental filter for bryophyte community assembly over the landscape. Sites with low atmospheric VPD, hosting simultaneously rare as well as widespread bryophytes, thus represent hotspots of bryophyte diversity in the landscape. Our findings of dominant temperature control on VPD variability across the landscape suggest that even the sites which can be considered as buffered against climate warming because of locally higher actual vapor pressure will be negatively affected by warming. With climate warming, areas with low VPD will likely shrink, and their bryophyte diversity will become more vulnerable (Pardow and Lakatos, 2013). Moreover, the increasingly frequent and severe canopy disturbances will likely further increase understory temperatures and therefore consequently also VPD (Wolf et al., 2021; Máliš et al., 2023). Our results suggest that such changes will reshuffle bryophyte communities, supporting widespread mesic bryophytes at the expense of regionally rare species near their distributional limits. Such changes will likely decrease not only local and regional bryophyte species richness but also trigger biotic homogenization of bryophyte assemblages across larger spatial scales (Staude et al., 2020).

#### 4.3 Disentangling atmospheric VPD and temperature

454

455 The close coupling between VPD and maximum temperature across the landscape clearly shows the need – and 456 simultaneously the difficulty – of disentangling the influences of VPD and temperature on plant communities. 457 While temperature affects basic life functions of bryophytes like photosynthesis, respiration (Dilks and Proctor, 1975), and growth (Furness and Grime, 1982), bryophytes thrive in a wide range of temperatures - from less than 458 459 -30 °C (Dilks and Proctor, 1975) to over 40 °C in a dry state (Hearnshaw and Proctor, 1982). For most bryophytes, the optimal growth temperature ranges from 12 to 25 °C (Vanderpoorten and Goffinet, 2009). However, many 460 bryophyte species grow even at temperatures around 5 °C (Dilks and Proctor, 1975), and some can even 461 462 photosynthesize at temperatures below 0 °C (Lösch et al., 1983). Therefore, temperature is hardly a direct limiting 463 factor of bryophyte distribution and community composition in temperate regions. 464 Our results fully support this conclusion, as we found that mean VPD was much better predictor of bryophyte community composition and richness than maximum temperature or maximum VPD. Bryophytes probably survive 465 466 the most extreme conditions represented by maximum VPD in desiccated state. However, the time required to 467 recover from desiccation increases and degree of recovery decreases with the length of desiccation (Proctor, Oliver et al., 2007). Bryophytes are therefore probably more sensitive to time-averaged characteristics of site 468 microclimatic condition than to short-term extremes captured by maximum VPD. The open question is whether 469 470 these findings apply also to vascular plants, which cannot survive microclimatic extremes in desiccated state and 471 can be therefore more sensitive to the microclimatic extremes (Schönbeck et al., 2022). 472 Several studies of vascular plants have attempted to distinguish the independent effect of VPD from other 473 microclimatic factors affecting plant functioning and distribution (Eamus et al., 2013; Denham et al., 2021; Flo et al., 2022; Fu et al., 2022; Kopecký et al., 2024), highlighting the critical importance of VPD (Novick et al., 2016; 474 475 Schönbeck et al., 2022). Unfortunately, no physiological studies addressed the independent effects of VPD on bryophytes, despite clear indications that VPD plays a key role (Busby et al., 1978; Sonnleitner et al., 2009). 476 477 So far, studies of bryophyte physiology concentrated on desiccation tolerance (Morales-Sánchez et al., 2022). 478 While desiccation tolerance is an adaptation to cope with the external lack of water, the ultimate driver of 479 desiccation is atmospheric VPD. A deeper focus on atmospheric VPD can therefore bring a new insight into 480 bryophyte ecology and distribution.

#### 5. Conclusions

481

482

483 484

485

486

487

488

489

490

491

Atmospheric VPD controls community composition, and richness and structure of bryophyte assemblages in temperate forest understory. Even across the landscape with extremely rugged terrain, spatial variability in atmospheric VPD was controlled by temperature-dependent saturated vapor pressure. Maximum air temperature and VPD are thus tightly coupled at biologically relevant scales and their effects are hard to disentangle. Nevertheless, we found that the time-averaged mean VPD was much better predictor of bryophyte assemblages than maximum temperature (or closely related maximum VPD) representing microclimatic extremes. This points toward the mean atmospheric VPD as the most important variable representing time-averaged evaporative stress and highlights so far overlooked importance of atmospheric VPD for bryophyte community ecology and distribution, both ecological and physiological studies suggest that bryophytes in temperate zone are not directly limited by temperature (Dilks and Proctor, 1975; Furness and Grime, 1982) but rather by evaporative stress

represented by VPD (Busby et al., 1978; Dilks and Proctor, 1979). With climate warming, the tight coupling between VPD and local air temperature will cause nonlinear increases in VPD-driven evaporative stress, which will subsequently reshuffle bryophyte community composition and decrease species richness. Especially vulnerable will be azonally occurring bryophyte species occurring near their distributional range limits concentrated in microclimatic refugia with low VPD.

#### Appendix A

#### VPD variability over the summer season

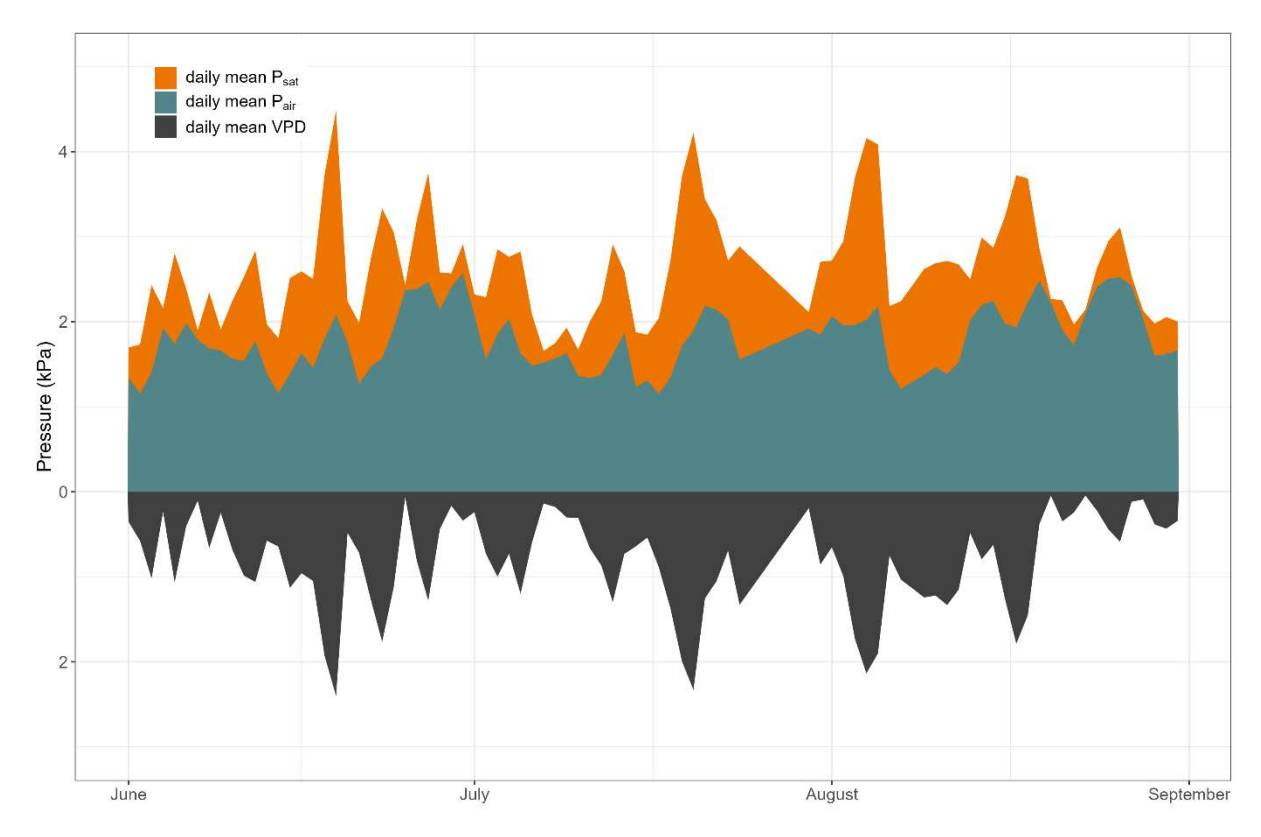


Figure A1: Daily values of maximum vapor pressure deficit (VPD) and corresponding values of saturated (Psat) and actual (Pair) vapor pressures, averaged over 38 permanent vegetation plots during June-August 2022.

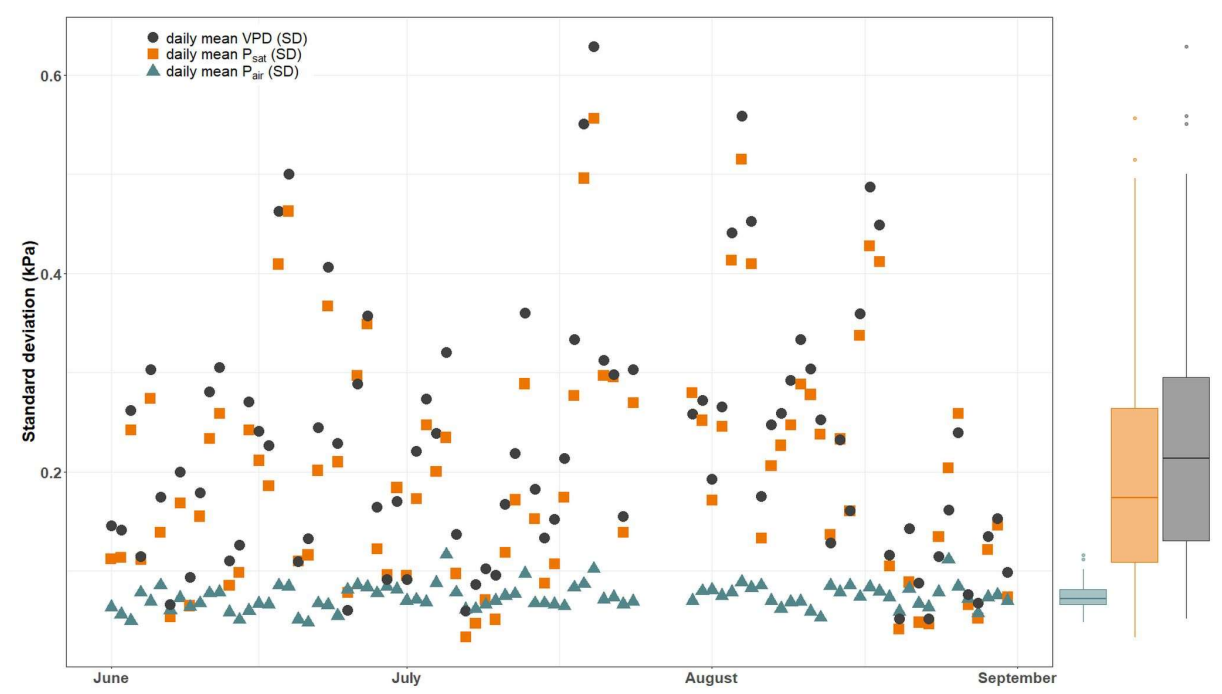


Figure A2: Spatial variability of VPD (black circles) is tightly coupled with the spatial variability in  $P_{\text{sat}}$  (orange squares) but not with  $P_{\text{air}}$  (blue triangles). Each data point shows the standard deviation of the daily value measured at 38 study sites. Marginal boxplots summarize spatial variability (daily standard deviations) during the growing season (June August 2022).

#### Correlation of variables representing evaporative stress and its components

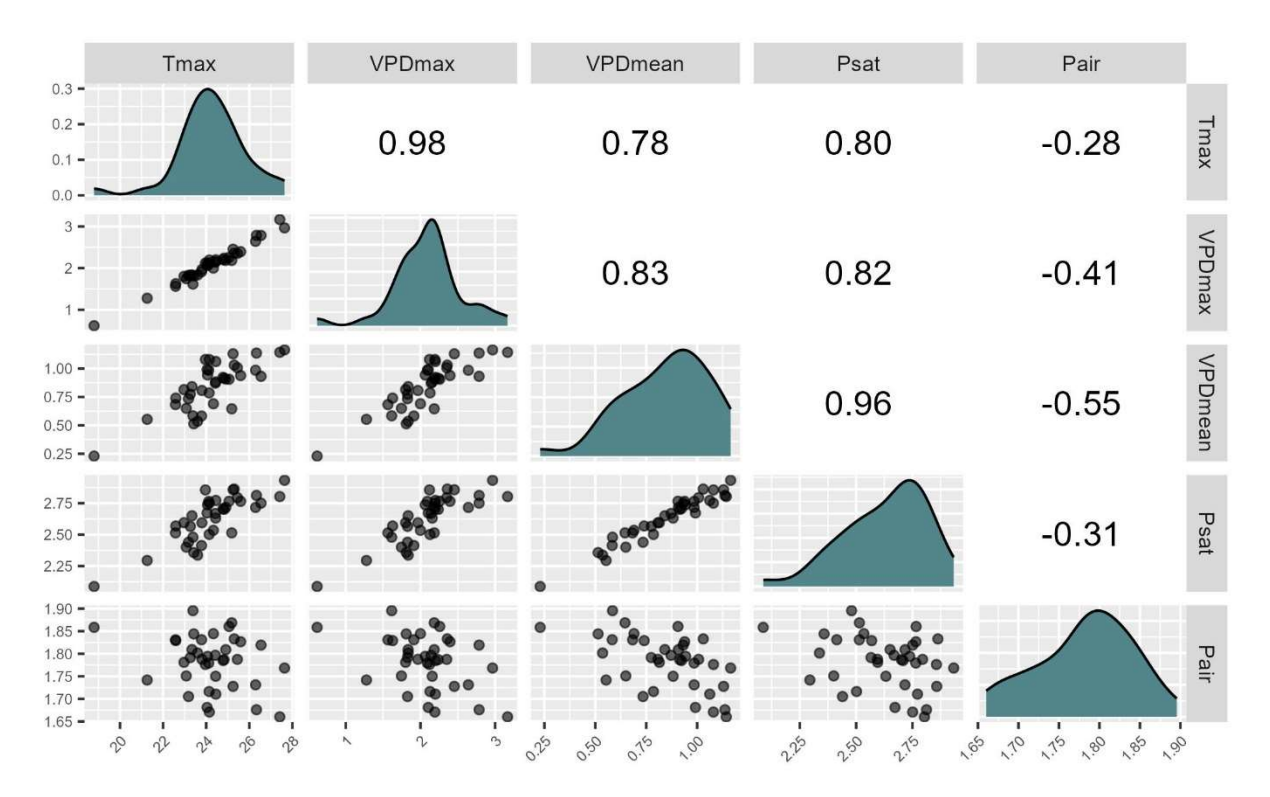


Figure A1: Pearson correlation matrix of microclimatic variables representing evaporative stress (maximum temperature, maximum and mean VPD) and its components (mean  $P_{\text{sat}}$  and mean  $P_{\text{air}}$ ).

509 Appendix B 510 VPD estimate from in-situ air temperature and regional air humidity 511 Based on our results, we speculated that local atmospheric VPD can be reasonably estimated using the in-situ air 512 temperature measurements paired with relative air humidity measurements representative for the whole region 513 (and therefore the same for all plots situated within that region). 514 To explore this idea, we estimated the average daily maximum atmospheriemean VPD using in-situ measured air 515 temperature (HOBO U23 ProV2 dataloggers in 1.5 m height) and relative air humidity measured in the Tokáň 516 weather station located in the study area (Fig. 1). 517 While the measured and estimated VPD were closely correlated (Pearson R= 0.9897), estimated VPD tended to 518 bewere consistently higher than in-situ measured VPD (Fig. B1). 519 Therefore, we conclude that the relative position of the site on the VPD gradient can be reasonably estimated from 520 in-situ microclimate temperature measurements paired with regional relative air humidity measurements. 521 However, this approach does not provide a reliable estimate of local atmospheric VPD, especially on sites with 522 locally higher air humidity.it should be stressed that this approach generates VPD estimates which provide reasonable ranking of the sites along the VPD gradient, but generally overestimate the VPD (Fig. B1), likely 523 because it does not account for locally higher actual vapor pressure, for example near springs, water bodies or on 524 525 permanently waterlogged soils. Therefore, this approach cannot fully replace local air humidity measurements.

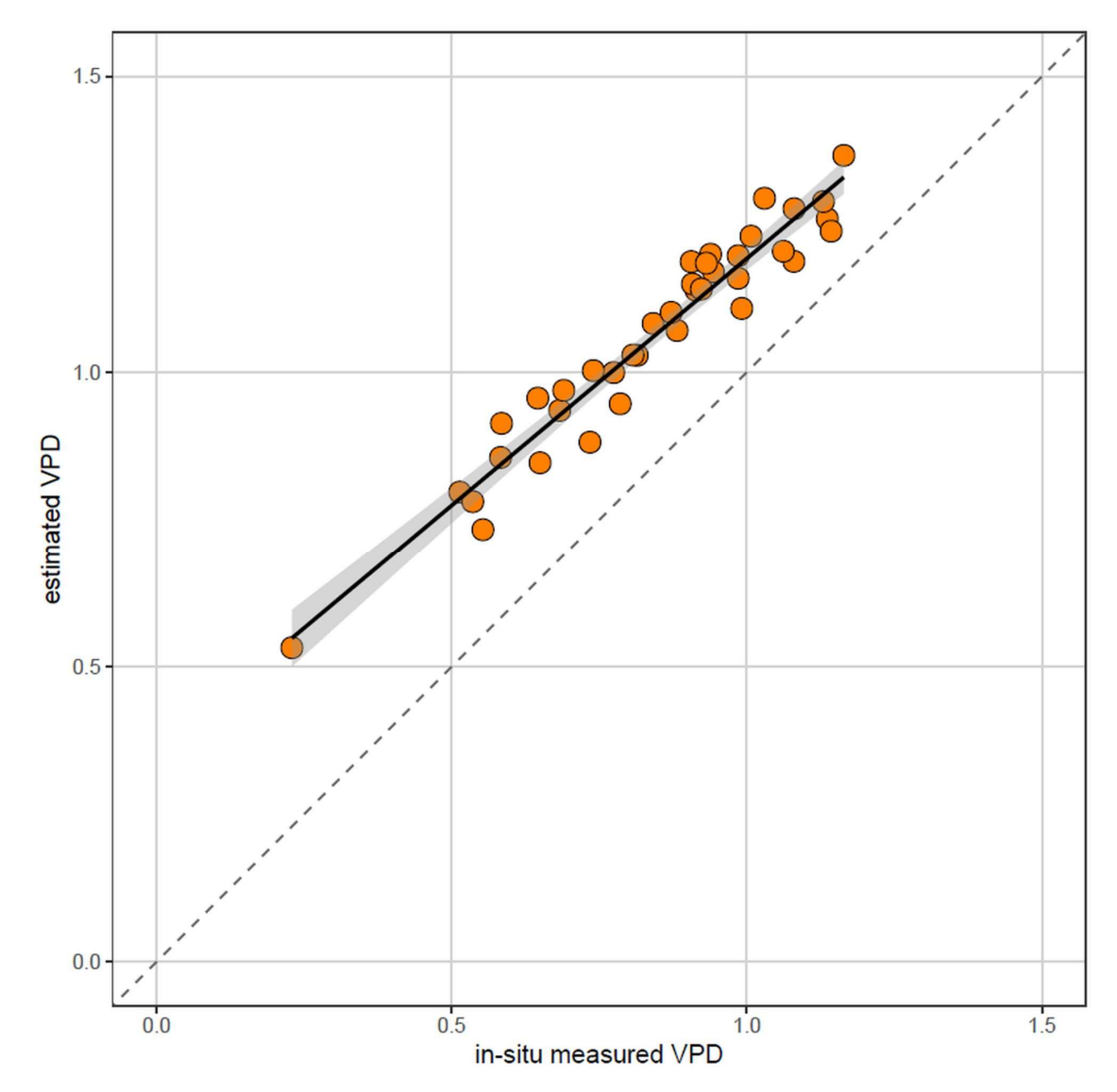


Figure B1: Relationship between in-situ measured average daily maximum mean VPD and average daily maximum mean VPD estimated from in-situ measured air temperature and relative air humidity measured in regional weather station (June-August 2022). While the measured and estimated VPD are closely correlated (Pearson R = 0.9897), estimated VPD tends to be higher than in-situ measured VPD, likely because of locally higher air humidity in topographically sheltered sites near valley bottoms.

#### Appendix C

List of bryophyte species, their occurrence and biogeographical affinity

Table C1: Complete species list of bryophyte species recorded at 38 study plots. Biogeographical categories follow Hill and Preston (1998).

Spe	ecies name	Occurence	Taxonomic group
1 Die	cranum scoparium	32	moss
<b>2</b> Let	ucobryum juniperoideum	26	moss
<b>3</b> Hy	pnum cupressiforme	24	moss
<b>4</b> Te	traphis pellucida	21	moss
5 Ba	zzania trilobata	18	liverwort

6	Polytrichum formosum	17	moss
7	Lophocolea heterophyllaChiloscyphus	15	liverwort
0	profundus	1.5	
8	Plagiothecium laetum/curvifolium	15	moss
9	Orthodontium lineare	13	moss
10	Plagiothecium undulatum	11	moss
11	Pleurozium schreberi	10	moss
12	Sphagnum girgensohnii/capillifolium	10	moss
12	Sphaghum girgensonnu/capititjoitum	10	moss
13	Dicranodontium denudatum	9	moss
1.4	C	0	
14	Campylopus flexuosus	8	moss
15	Lepidozia reptans	8	liverwort
16	Lophocolea bidentata Chiloscyphus cuspidatus	8	liverwort
17	Pohlia nutans	8	moss
18	Mnium hornum	7	moss
19	Calypogeia integristipula	6	liverwort
20	Herzogiella seligeri	5	moss
21	Brachythecium rutabulum	4	moss
22	Calypogeia mulleriana	4	liverwort
23	Dicranella heteromalla	4	moss
24	Orthodicranum montanum	4	moss
25		2	11
25	Mylia taylorii	3	liverwort
26	Atrichum undulatum	2	moss
27	Dicranum majus	2	moss
28	Odontoschisma denudatum	2	liverwort
29	Pellia epiphylla	2	liverwort
30	Polytrichum commune	2	moss
31	Ptilidium ciliare	2	liverwort
32	Cephalozia bicuspidata	1	liverwort
33	Dicranoweisia cirrata	1	moss
34	Lophozia ventricosa	1	liverwort
35	Plagiomnium affine	1	moss
36	Plagiomnium undulatum	1	moss
37	Rhabdoweisia fugax	1	moss
38	Riccardia multifida	1	liverwort
39	Scapania nemorea	1	liverwort
3)	Soupaina nemorea	•	11.01 11.011

Data availability. The data supporting the findings of this study are currently provided for peer review on GitHub public repository (<a href="https://doi.org/10.5281/zenodo.15805801">https://doi.org/10.5281/zenodo.15805801</a>).

- Author contribution. Conceptualization: AR, MMan, MMac, JW, MK. Funding acquisition: MK. Data curation:
- AR. Methodology: MMac, MK. Formal analysis: AR. Investigation: AR, MMan, MMac, JW, MK. Visualization:
- AR, MMan, MMac, MK. Writing original draft: AR. Writing review & editing: AR, MMan, MMac, JW, MK.
- 541 Supervision: MK.
- 542 Competing interest. The authors declare that they have no conflict of interest.
- 543 Acknowledgements. We thank all colleagues who helped us to collect microclimate data, . We also thank
- 544 the Administration of the Bohemian Switzerland National Park for their the long-term support, and Caroline
- 545 Greiser, Alain Vanderpoorten and anonymous reviewer for their useful comments and suggestions.
- 546 Financial support. This study was supported by the Czech Science Foundation (project GACR 23-06614S) and
- the Czech Academy of Sciences (project RVO 67985939).

#### References

- Almeida-Neto, M., Guimaraes, P., Guimaraes, P. R. J., Loyola, R. D., and Ulrich, W.: A consistent metric for
- nestedness analysis in ecological systems: reconciling concept and measurement, Oikos, 117,
- 551 1227–1239, https://doi.org/10.1111/j.2008.0030-1299.16644.x, 2008.
- Anderson, D. B.: Relative humidity or vapor pressure deficit, Ecology, 17(2), 277-282,
- 553 <u>https://doi.org/10.2307/1931468, 1936.</u>
- Ashcroft, M. B. and Gollan, J. R.: Moisture, thermal inertia, and the spatial distributions of near-surface soil
- and air temperatures: understanding factors that promote microrefugia, Agr. Forest Meteorol.,
- 556 176, 77–89, https://doi.org/10.1016/j.agrformet.2013.03.008, 2013.
- Breshears, D. D., Adams, H. D., Eamus, D., McDowell, N. G., Law, D. J., Will, R. E., Williams, A. P., and
- Zou, C. B.: The critical amplifying role of increasing atmospheric moisture demand on tree
- mortality and associated regional die-off, Front. Plant Sci., 4, 2–5,
- 560 <u>https://doi.org/10.3389/fpls.2013.00266, 2013.</u>
- Buck, A. L.: New equations for computing vapor pressure and enhancement factor. J. Appl. Meteorol. Clim.,
- 562 20(12), 1527–1532, <a href="https://doi.org/10.1175/1520-0450(1981)020<1527:NEFCVP>2.0.CO;2">https://doi.org/10.1175/1520-0450(1981)020<1527:NEFCVP>2.0.CO;2</a>,
- 563 1981.
- Buck, A. L.: Buck research manual, 1996.
- Busby, J. R., Bliss, L. C., and Hamilton, C. D.: Microclimate control of growth rates and habitats of the boreal
- forest mosses, *Tomenthypnum nitens* and *Hylocomium splendens*, Ecol. Monogr., 48(2), 95–110,
- 567 <u>https://doi.org/10.2307/2937294</u>, 1978.
- Busby, J. R. and Whitfield, D. W. A.: Water potential, water content, and net assimilation of some boreal
- forest mosses, Can. J. Botany, 56(13), 1551–1558, <a href="https://doi.org/10.1139/b78-184">https://doi.org/10.1139/b78-184</a>, 1978.
- Campbell, G. S. and Norman, J. M.: An introduction to environmental biophysics, 2nd ed., Springer, New
- 571 York, 286 pp., https://doi.org/10.1007/978-1-4612-1626-1, 1998.
- Dahlberg, C. J., Ehrlén, J., Christiansen, D. M., Meineri, E., and Hylander, K.: Correlations between plant
- 573 climate optima across different spatial scales, Environ. Exp. Botany, 170, 103899,
- 574 <u>https://doi.org/10.1016/j.envexpbot.2019.103899, 2020.</u>

- 575 Davis, K. T., Dobrowski, S. Z., Holden, Z. A., Higuera, P. E., and Abatzoglou, J. T.: Microclimatic buffering 576 in forests of the future: the role of local water balance, Ecography, 42(1), 1–11, https://doi.org/10.1111/ecog.03836, 2019. 577 Denham, S. O., Oishi, A. C., Miniat, C. F., Wood, J. D., Yi, K., Benson, M. C., and Novick, K. A.: Eastern US 578 579 deciduous tree species respond dissimilarly to declining soil moisture but similarly to rising 580 evaporative demand, Tree Physiol., 41(6), 1-56, https://doi.org/10.1093/treephys/tpaa153, 2021. Dilks, T. J. K. and Proctor, M. C. F: Comparative experiments on temperature responses of bryophytes: 581 582 assimilation, respiration and freezing damage, J. Bryol., 8(3), 317-336, 583 https://doi.org/10.1179/jbr.1975.8.3.317, 1975. 584 Dilks, T. J. K. and Proctor, M. C. F.: Photosynthesis, respiration and water content in bryophytes, New 585 Phytol., 82(1), 97–114, https://doi.org/10.1111/j.1469-8137.1979.tb07564.x, 1979. 586 Dobrowski, S. Z.: A climatic basis for microrefugia: the influence of terrain on climate, Global Change Biol., 587 17(2), 1022–1035, https://doi.org/10.1111/j.1365-2486.2010.02263.x, 2011. 588 Eamus, D., Boulain, N., Cleverly, J., and Breshears, D. D.: Global change-type drought-induced tree 589 mortality: vapor pressure deficit is more important than temperature per se in causing decline in 590 tree health, Ecol. Evol., 3(8), 2711–2729, https://doi.org/10.1002/ece3.664, 2013. 591 Feld, S. I., Cristea, N. C. and Lundquist, J. D.: Representing atmospheric moisture content along mountain 592 slopes: examination using distributed sensors in the Sierra Nevada, California, Water Resour. 593 Res., 49, 4424–4441, 2013. 594 Fenton, N. J. and Frego, K. A.: Bryophyte (moss and liverwort) conservation under remnant canopy in 595 managed forests, Biol. Conserv., 122(3), 417-430, https://doi.org/10.1016/j.biocon.2004.09.003, 596 2005. 597 Finocchiaro, M., Médail, F., Saatkamp, A., Diadema, K., Pavon, D., Brousset, L., and Meineri, E.: 598 Microrefugia and microclimate: unraveling decoupling potential and resistance to heatwaves, 599 Sci. Total Environ., 924, 171696, https://doi.org/10.1016/j.scitotenv.2024.171696, 2024. 600 Flo, V., Martínez-Vilalta, J., Granda, V., Mencuccini, M., and Poyatos, R.: Vapour pressure deficit is the main 601 driver of tree canopy conductance across biomes, Agr. Forest Meteorol., 322, 109029, https://doi.org/10.1016/j.agrformet.2022.109029, 2022. 602 603 Fu, Z., Ciais, P., Prentice, I. C., Gentine, P., Makowski, D., Bastos, A., Luo, X., Green, J. K., Stoy, P. C., 604 Yang, H., and Hajima, T.: Atmospheric dryness reduces photosynthesis along a large range of soil water deficits, Nat. Commun., 13(1), 1–10, https://doi.org/10.1038/s41467-022-28652-7, 605 2022. 606 607 Furness, S. B. and Grime, J. P.: Growth rate and temperature responses in bryophytes: II. A comparative study of species of contrasted ecology, J. Ecol., 70(2), 525–536, https://doi.org/10.2307/2259920, 608
- pp., ISBN 978-0-521-69322-6, 2009.
  Grossiord, C., Buckley, T. N., Cernusak, L. A., Novick, K. A., Poulter, B., Siegwolf, R. T. W., Sperry, J. S.,
  and McDowell, N. G.: Plant responses to rising vapor pressure deficit, New Phytol., 226(6),
  1550–1566, https://doi.org/10.1111/nph.16485, 2020.

609

610

1982.

Goffinet, B. and Shaw, J. A. (Eds.): Bryophyte biology, 2nd ed., Cambridge University Press, New York, 556

613	Hartel, H., Sadio, J., Swierkosz, K., and Markova, I.: Phytogeography of the sandstone areas in the Bonemian
616	Cretaceous Basin (Czech Republic/Germany/Poland), in: Sandstone landscapes, edited by:
617	Härtel, H., Cílek, V., Herben, T., Jackson, A., and Williams, R., Academia, Praha, 177-189,
618	https://doi.org/10.6084/m9.figshare.92598, 2007.
619	Hearnshaw, G. F. and Proctor, M. C. F.: The effect of temperature on the survival of dry bryophytes, New
620	Phytol., 90(2), 221–228, https://doi.org/10.1111/j.1469-8137.1982.tb03254.x, 1982.
621	Hill, M. O. and Preston, C. D.: The geographical relationships of British and Irish bryophytes, J. Bryol., 20(1)
622	127–226, https://doi.org/10.1179/jbr.1998.20.1.127, 1998.
623	Hinshiri, H. M. and Proctor, M. C. F.: The effect of desiccation on subsequent assimilation and respiration of
624	the bryophytes Anomodon viticulosus and Porella platyphylla, New Phytol., 70(3), 527-538,
625	https://doi.org/10.1111/j.1469-8137.1971.tb02554.x, 1971.
626	Hjort, J., Heikkinen, R. K., and Luoto, M.: Inclusion of explicit measures of geodiversity improve biodiversity
627	models in boreal landscape, Biodivers. Conserv., 21, 3487-3506,
628	https://doi.org/10.1007/s10531-012-0376-1, 2012.
629	IPCC: Climate Change 2023: synthesis report, <a href="https://doi.org/10.59327/IPCC/AR6-9789291691647">https://doi.org/10.59327/IPCC/AR6-9789291691647</a> , 2023.
630	Johnston, M. R, Barnes, M. L., Preisler, Y., Smith, W. K., Biederman, J. A., Scott, R. L., Williams, A. P., and
631	Dannenberg, M. P.: Effects of hot versus dry vapor pressure deficit on ecosystem carbon and
632	water fluxes, J. Geophys. ResBiogeo., 130(1), e2024JG008146,
633	https://doi.org/10.1029/2024JG008146, 2025.
634	Jones, H. G.: Plants and microclimate: a quantitative approach to environmental plant physiology, 3rd ed.,
635	Cambridge University Press, <a href="https://doi.org/10.1017/CBO9780511845727">https://doi.org/10.1017/CBO9780511845727</a> , 2014.
636	Kopecký, M., Hederová, L., Macek, M., Klinerová, T., and Wild, J.: Forest plant indicator values for moisture
637	reflect atmospheric vapour pressure deficit rather than soil water content, New Phytol., 244(5),
638	1801-1811., https://doi.org/10.1111/nph.20068, 2024.
639	Kučera, J., Váňa, J., and Hradílek. Z.: Bryophyte flora of the Czech Republic: updated checklist and Red List
640	and a brief analysis, Preslia, 84(3), 813–850, 2012.
641	Lawrence, M. G.: The relationship between relative humidity and the dewpoint temperature in moist air: a
642	simple conversion and applications, B. Am. Meteorol. Soc., 86(2), 225-234,
643	https://doi.org/10.1175/BAMS-86-2-225, 2005.
644	Legendre, P.: Studying beta diversity: ecological variation partitioning by multiple regression and canonical
645	analysis, J. Plant Ecol.,1(1), 3–8, <a href="https://doi.org/10.1093/jpe/rtm001">https://doi.org/10.1093/jpe/rtm001</a> , 2008.
646	Legendre, P., Oksanen, J., and ter Braak, C. J. F.: Testing the significance of canonical axes in redundancy
647	analysis, Methods Ecol. Evol., 2(3), 269–277, https://doi.org/10.1111/j.2041-
648	<u>210X.2010.00078.x</u> , 2011.
649	Lembrechts, J. J., Aalto, J., Ashcroft, M. B., et al.: SoilTemp: a global database of near-surface temperature,
650	Glob. Change Biol., 26(11), 6616–6629, <a href="https://doi.org/10.1111/gcb.15123">https://doi.org/10.1111/gcb.15123</a> , 2020.
651	Lennon, J. J., Koleff, P., Greenwood, J. J. D., and Gaston, K. J.: The geographical structure of British bird
652	distributions: diversity, spatial turnover and scale, J. Anim. Ecol., 70(6), 966-979,
653	https://doi.org/10.1046/j.0021.8790.2001.00563.v2001

654	León-Vargas, Y., Engwald, S., and Proctor, M. C. F.: Microclimate, light adaptation and desiccation tolerance
655	of epiphytic bryophytes in two Venezuelan cloud forests, J. Biogeogr., 33(5), 901-913,
656	https://doi.org/10.1111/j.1365-2699.2006.01468.x, 2006.
657	López, J., Way, D. A., and Sadok, W.: Systemic effects of rising atmospheric vapor pressure deficit on plant
658	physiology and productivity, Glob. Change Biol., 27(9), 1704-1720,
659	https://doi.org/10.1111/gcb.15548, 2021.
660	Lösch, R., Kappen, L., and Wolf, A.: Productivity and temperature biology of two snowbed bryophytes, Polar
661	Biol., 1(4), 243–248, https://doi.org/10.1007/BF00443195, 1983.
662	Lu, H., Qin, Z., Lin, S., Chen, X., Chen, B., He, B., Wei, J., and Yuan, W.: Large influence of atmospheric
663	vapor pressure deficit on ecosystem production efficiency, Nat. Commun., 13(1), 10-13,
664	https://doi.org/10.1038/s41467-022-29009-w, 2022.
665	Macek, M., Kopecký, M., and Wild, J.: Maximum air temperature controlled by landscape topography affects
666	plant species composition in temperate forests, Landscape Ecol., 34, 2541-2556,
667	https://doi.org/10.1007/s10980-019-00903-x, 2019.
668	Máliš, F., Ujházy, K., Hederová, L., Ujházyová, M., Csölleová, L., Coomes, D. A., and Zellweger, F.:
669	Microclimate variation and recovery time in managed and old-growth temperate forests, Agr.
670	Forest Meteorol., 342, 109722, <a href="https://doi.org/10.1016/j.agrformet.2023.109722">https://doi.org/10.1016/j.agrformet.2023.109722</a> , 2023.
671	Man, M., Kalčík, V., Macek, M., Brůna, J., Hederová, L., Wild, J., and Kopecký, M.: myClim: microclimate
672	data handling and standardised analyses in R, Methods Ecol. Evol., 14(9), 2308-2320,
673	https://doi.org/10.1111/2041-210X.14192, 2023.
674	Man, M., Wild, J., Macek, M., and Kopecký, M.: Can high-resolution topography and forest canopy structure
675	substitute microclimate measurements? Bryophytes say no., Sci. Total Environ., 821, 153377,
676	https://doi.org/10.1016/j.scitotenv.2022.153377, 2022.
677	Marková, I.: Mechorosty Českého Švýcarska (Labských pískovců), in: Labské pískovce - historie, příroda a
678	ochrana území, edited by: Bauer, P., Kopecký, V., and Šmucar, J., Agentura ochrany přírody
679	a krajiny ČR, Správa CHKO Labské pískovce, Děčín, 106-120, 2008. [in Czech language]
680	Merinero, S., Dahlberg, C. J., Ehrlén, J., and Hylander, K.: Intraspecific variation influences performance
681	of moss transplants along microclimatic gradients, Ecology, 101(5), e02999,
682	https://doi.org/10.1002/ecy.2999, 2020.
683	McArdle, B. H. and Anderson, M. J.: Fitting multivariate models to community data: a comment on distance-
684	based redundancy analysis, <i>Ecology</i> , 82(1), 290–297, <a href="https://doi.org/10.1890/0012-">https://doi.org/10.1890/0012-</a>
685	9658(2001)082[0290:FMMTCD]2.0.CO;2, 2001.
686	McDowell, N., Pockman, W. T., Allen, C. D., Breshears, D. D., Cobb, N., Kolb, T., Plaut, J., Sperry, J., West,
687	A., Williams, D. G., and Yepez, E. A.: Mechanisms of plant survival and mortality during
688	drought: why do some plants survive while others succumb to drought?, New Phytol., 178(4),
689	719–739, <a href="https://doi.org/10.1111/j.1469-8137.2008.02436.x">https://doi.org/10.1111/j.1469-8137.2008.02436.x</a> , 2008.
690	Morales-Sánchez, J. Á. M., Mark, K., Souza, J. P.S., and Niinemets, Ü.: Desiccation - rehydration
691	measurements in bryophytes: current status and future insights, J. Exp. Bot., 73(13), 4338-4361
692	https://doi.org/10.1093/jxb/erac172, 2022.

Novick, K. A., Ficklin, D. L., Grossiord, C., Konings, A. G., Martínez-Vilalta, J., Sadok, W., Trugman, A. T., Williams, A. P., Wright, A. J., Abatzoglou, J. T., Dannenberg, M. P., Gentine, P., Guan, K., Johnston, M. R., Lowman, L. E. L., Moore, D. J. P., and McDowell, N. G.: The impacts of rising vapour pressure deficit in natural and managed ecosystems, Plant Cell Environ., 47(9),

3561-3589, https://doi.org/10.1111/pce.14846, 2024.

- Novick, K. A., Ficklin, D. L., Stoy, P. C., Williams, C. A., Bohrer, G., Oishi, A. C., Papuga, S. A., Blanken, P. D., Noormets, A., Sulman, B. N., Scott, R. L., Wang, L., and Phillips, R. P.: The increasing importance of atmospheric demand for ecosystem water and carbon fluxes, Nat. Clim. Change, 6(11), 1023–1027, https://doi.org/10.1038/nclimate3114, 2016.
- Ogée, J., Walbott, M., Barbeta, A., Corcket, E., and Brunet, Y.: Decametric-scale buffering of climate extremes in forest understory within a riparian microrefugia: the key role of microtopography, Int. J. Biometeorol., 68(9), 1741–1755, https://doi.org/10.1007/s00484-024-02702-9, 2024.
- Oksanen, J., Simpson, G., Blanchet, F., Kindt, R., Legendre, P., Minchin, P. R., O'Hara, R. B., Solymos, P.,
  Stevens, M. H. H., Szoecs, E., Wagner, H., Barbour, M., Bedward, M., Bolker, B., Borcard, D.,
  Carvalho, G., Chirico, M., De Caceres, M., Durand, S., Evangelista, H. B. A., FitzJohn, R.,
  Friendly, M., Furneaux, G., Hill, M. O., Lahti, L., McGlinn, D., Ouellette, M-H., Cunha, E. R.,
  Smith, T., Stier, A., ter Braak, C. J. F., Weedon, J., and Borman, T.: vegan: Community
  Ecology Package [R package vegan version 2.6-4], <a href="https://cran.r-project.org/package=vegan">https://cran.r-project.org/package=vegan</a>,
  5 Feb. 2025, 2022.
- Oliver, M. J. and Bewley, J. D.: Plant desiccation and protein synthesis, Plant Physiol., 74(4), 923–927, https://doi.org/10.1104/pp.74.4.923, 1984.
- Oliver, M. J., Velten, J., and Wood, A. J.: Bryophytes as experimental models for the study of environmental stress tolerance: *Tortula ruralis* and desiccation-tolerance in mosses, Plant Ecol., 151(1), 73–84, <a href="https://doi.org/10.1023/A:1026598724487">https://doi.org/10.1023/A:1026598724487</a>, 2000.
- Pardow, A. and Lakatos, M.: Desiccation tolerance and global change: implications for tropical bryophytes in lowland forests, Biotropica, 45(1), 27–36, <a href="https://doi.org/10.1111/J.1744-7429.2012.00884.X">https://doi.org/10.1111/J.1744-7429.2012.00884.X</a>, 2013.
- Pedersen, T. and Crameri, F.: scico: Colour palettes based on the scientific colour maps [R package scio version 1.5.0], <a href="https://cran.reproject.org/package=scico">https://cran.reproject.org/package=scico</a>, 11 Mar. 2025, 2023.
- Peres-Neto, P. R., Legendre, P., Dray, S., and Borcard D.: Variation partitioning of species data matrices:

  estimation and comparison of fractions, Ecology, 87, 2614–25, https://doi.org/10.1890/0012-9658(2006)87[2614:VPOSDM]2.0.CO;2, 2006.
- Platt, K. A., Oliver, M. J., and Thomson, W. W.: Membranes and organelles of dehydrated *Selaginella* and *Tortula* retain their normal configuration and structural integrity: freeze fracture evidence,
  Protoplasma, 178(1–2), 57–65, <a href="https://doi.org/10.1007/BF01404121">https://doi.org/10.1007/BF01404121</a>, 1994.
- Proctor, M. C. F. The bryophyte paradox: tolerance of dessication, evasion of drought, Plant Ecol., 151(1), 41–49, https://doi.org/10.1023/A:1026517920852, 2000.
- Proctor, M. C. F. Patterns of desiccation tolerance and recovery in bryophytes, Plant Growth Regul., 35(2), 147–156, <a href="https://doi.org/10.1023/A:1014429720821">https://doi.org/10.1023/A:1014429720821</a>, 2001.

732	Proctor, M. C. F., Ligrone, R., and Duckett, J. G.: Desiccation tolerance in the moss <i>Polytrichum formosum</i> :
733	physiological and fine-structural changes during desiccation and recovery, Ann. BotLondon,
734	99(1), 75–93, https://doi.org/10.1093/aob/mc1246, 2007.
735	Proctor, M. C. F, Oliver, M. J., Wood, A. J., and Alpert, P.: Desiccation-tolerance in bryophytes: a review,
736	Bryologist, 110(4), 595–621, https://doi.org/10.1639/0007-
737	2745(2007)110[595:DIBAR]2.0.CO;2, 2007.
738	R Core Team: R: A language and environment for statistical computing, R foundation for statistical
739	computing, Vienna, Austria, <a href="https://www.R-project.org/">https://www.R-project.org/</a> , 15 Mar. 2025, 2024.
740	Rambo, T. R. and Muir, P. S.: Forest floor bryophytes of Pseudotsuga menziesii-Tsuga heterophylla stands in
741	Oregon: influence of substrate and overstory, Bryologist, 101(1), 116-130,
742	https://doi.org/10.2307/3244083, 1998.
743	Rice, S. K., Collins, D., and Anderson, A. M.: Functional significance of variation in bryophyte canopy
744	structure, Am. J. Bot., 88(9), 1568–1576, https://doi.org/10.2307/3558400, 2001.
745	Ruehr, N. K., Law, B. E., Quandt, D., and Williams, M.: Effects of heat and drought on carbon and water
746	dynamics in a regenerating semi-arid pine forest: a combined experimental and modelling
747	approach, Biogeosciences, 11, 4139-4156, <a href="https://doi.org/10.5194/bg-11-4139-2014">https://doi.org/10.5194/bg-11-4139-2014</a> , 2014.
748	Schmalholz, M. and Hylander, K.: Microtopography creates small-scale refugia for boreal forest floor
749	bryophytes during clear-cut logging, Ecography, 34(4), 637–348,
750	https://doi.org/10.1111/j.1600-0587.2010.06652.x, 2011.
751	Schofield, W. B.: Ecological significance of morphological characters in the moss gametophyte, Bryologist,
752	84(2), 149–165, <a href="https://doi.org/10.2307/3242819">https://doi.org/10.2307/3242819</a> , 1981.
753	Schönbeck, L. C., Schuler, P., Lehmann, M. M., Mas, E., Mekarni, L., Pivovaroff, A. L., Turberg, P., and
754	Grossiord, C.: Increasing temperature and vapour pressure deficit lead to hydraulic damages in
755	the absence of soil drought, Plant, Cell Environ., 45(11), 3275-3289,
756	https://doi.org/10.1111/pce.14425, 2022.
757	Sonnleitner, M., Dullinger, S., Wanek, W., and Zechmeister, H.: Microclimatic patterns correlate with the
758	distribution of epiphyllous bryophytes in a tropical lowland rain forest in Costa Rica, J. Trop.
759	Ecol., 25(3), 321–330, <a href="https://doi.org/10.1017/S0266467409006002">https://doi.org/10.1017/S0266467409006002</a> , 2009.
760	Staude, I. R., Waller, D. M., Bernhardt-Römermann, M., Bjorkman, A. D., Brunet, J., De Frenne, P., Hédl, R.
761	Jandt, U., Lenoir, J., Máliš, F., Verheyen, K., Wulf, M., Pereira, H. M., Vangansbeke, P.,
762	Ortmann-Ajkai, A., Pielech, R., Berki, I., Chudomelová, M., Decocq, G., Dirnböck, T., Durak,
763	T., Heinken, T., Jaroszewicz, B., Kopecký, M., Macek, M., Malicki, M., Naaf, T., Nagel, T. A.,
764	Petřík, P., Reczyńska, K., Schei, F. H., Schmidt, W., Standovár, T., Świerkosz, K., Teleki, B.,
765	Van Calster, H., Vild, O., and Baeten, L.: Replacements of small- by large-ranged species scale
766	up to diversity loss in Europe's temperate forest biome, Nature, 4, 802-808,
767	https://doi.org/10.1038/s41559-020-1176-8, 2020.
768	Tetens, O.: Ueber einige meteorologische Begriffe. Zeitschrift für geophysik, 6, 297-309, 1930. [in German
769	language]
770	Ulrich, W., Almeida-Neto, M., and Gotelli, N. J.: A consumer's guide to nestedness analysis, Oikos, 118, 3-
771	17, https://doi.org/10.1111/j.1600-0706.2008.17053.x, 2009.

772 Vanderpoorten, A. and Engels, P.: The effects of environmental variation on bryophytes at regional scale, 773 Ecography, 25(5), 513-522, https://doi.org/10.1034/j.1600-0587.2002.250501.x, 2002. 774 Vanderpoorten, A. and Goffinet, B.: Introduction to bryophytes, Cambridge University Press, Cambridge, 303 pp., https://doi.org/10.1017/CBO9780511626838, 2009. 775 776 Vanwalleghem, T. and Meentemeyer, R. K.: Predicting forest microclimate in heterogeneous landscapes, 777 Ecosystems, 12, 1158–1172, https://doi.org/10.1007/s10021-009-9281-1, 2009. 778 Wagner, D.J. and Titus, J. E.: Comparative desiccation tolerance of two Sphagnum mosses, Oecologia, 62, 779 182-187, https://doi.org/10.1007/BF00379011, 1984. 780 Wei, L., Zhou, H., Link, T. E., Kavanagh, K. L., Hubbart, J. A., Du, E., Hudak, A. T., and Marshall, J. D.: 781 Forest productivity varies with soil moisture more than temperature in a small montane 782 watershed, Agr. Forest Meteorol., 259, 211-221, 783 https://doi.org/10.1016/j.agrformet.2018.05.012, 2018. 784 Wild, J., Macek, M., Kopecký, M., Zmeškalová, J., Hadincová, V., and Trachtová, P.: Temporal and spatial 785 variability of microclimate in sandstone landscape: detailed field measurement, in: Proceedings 786 of the 3rd International Conference on Sandstone Landscapes, Sandstone Landscapes, Diversity, Ecology and Conservation, University of Wroclaw, 220–224, 2013. 787 Will, R. E., Wilson, S. M., Zou, C. B., and Hennessey, T. C.: Increased vapor pressure deficit due to higher 788 789 temperature leads to greater transpiration and faster mortality during drought for tree seedlings 790 common to the forest-grassland ecotone, New Phytol., 200(2), 366–374, 791 https://doi.org/10.1111/nph.12321, 2013. 792 Williams, A. P., Allen, C. D., Macalady, A. K., Griffin, D., Woodhouse, C. A., Meko, D. M., Swetnam, T. W., 793 Rauscher, S. A., Seager, R., Grissino-Mayer, H. D., Dean, J. S., Cook, E. R., Gangodagamage, 794 C., Cai, M., and McDowell, N. G.: Temperature as a potent driver of regional forest drought 795 stress and tree mortality, Nat. Clim. Change, 3(3), 292–297, 796 https://doi.org/10.1038/nclimate1693, 2013. Wolf, K. D., Higuera, P. E., Davis, K. T., and Dobrowski, S. Z.: Wildfire impacts on forest microclimate vary 797 798 with biophysical context, *Ecosphere*, 12(5), e03467, https://doi.org/10.1002/ecs2.3467, 2021. 799 Wood, S. N.: Fast stable restricted maximum likelihood and marginal likelihood estimation of semiparametric 800 generalized linear models, J. R. Stat. Soc.: Series B (Statistical Methodology), 73(1), 3–36, 801 https://doi.org/10.1111/J.1467-9868.2010.00749.X, 2011. 802 Wörlen, C., Schulz, K., Huwe, B., and Eiden, R.: Spatial extrapolation of agrometeorological variables, Agr. 803 For. Meteorol., 94(3-4), 233-242, https://doi.org/10.1016/S0168-1923(99)00015-5, 1999. 804 Wright, D. H., Patterson, B. D., Mikkelson, G. M., Cutler, A., and Atmar, W.: A comparative analysis of 805 nested subset patterns of species composition, Oecologia, 113, 1–20, https://doi.org/10.1007/s004420050348, 1997. 806 Yuan, W., Zheng, Y., Piao, S., Ciais, P., Lombardozzi, D., Wang, Y., Ryu, Y., Chen, G., Dong, W., Hu, Z., 807 808 Jain, A. K., Jiang, C., Kato, E., Li, S., Lienert, S., Liu, S., Nabel, J. E. M. S., Qin, Z., Quine, T., 809 Sitch, S., Smith, W. K., Wang, F., Wu, C., Xiao, Z., and Yang, S.: Increased atmospheric vapor pressure deficit reduces global vegetation growth, Sci. Adv., 5(8), 1–13, 810

https://doi.org/10.1126/sciadv.aax1396, 2019.

Zeng, Q., Chen, X., Wood, A. J.: Two early light-inducible protein (ELIP) cDNAs from the resurrection plant *Tortula ruralis* are differentially expressed in response to desiccation, rehydration, salinity, and high light, J. Exp. Bot., 53(371), 1197–1205, <a href="https://doi.org/10.1093/jexbot/53.371.1197">https://doi.org/10.1093/jexbot/53.371.1197</a>, 2002.